

# GigaScience

## Multi-dimensional leaf phenotypes reflect root system genotype in grafted grapevine over the growing season --Manuscript Draft--

<b>Manuscript Number:</b>	GIGA-D-21-00137R2	
<b>Full Title:</b>	Multi-dimensional leaf phenotypes reflect root system genotype in grafted grapevine over the growing season	
<b>Article Type:</b>	Research	
<b>Funding Information:</b>	National Science Foundation (1546869)	Dr Allison J. Miller
<b>Abstract:</b>	<p>Background: Modern biological approaches generate volumes of multi-dimensional data, offering unprecedented opportunities to address biological questions previously beyond reach due to small or subtle effects. A fundamental question in plant biology is the extent to which below-ground activity in the root system influences above-ground phenotypes expressed in the shoot system. Grafting, an ancient horticultural practice that fuses the root system of one individual (the rootstock) with the shoot system of a second, genetically distinct individual (the scion), is a powerful experimental system to understand below-ground effects on above-ground phenotypes. Previous studies on grafted grapevines have detected rootstock influence on scion phenotypes including physiology and berry chemistry. However, the extent of the rootstock's influence on leaves, the photosynthetic engines of the vine, and how those effects change over the course of a growing season, are still largely unknown.</p> <p>Results: Here, we investigate associations between rootstock genotype and shoot system phenotypes using five multi-dimensional leaf phenotyping modalities measured in a common grafted scion: ionomics, metabolomics, transcriptomics, morphometrics, and physiology. Rootstock influence is ubiquitous but subtle across modalities with the strongest signature of rootstock observed in the leaf ionome. Moreover, we find that the extent of rootstock influence on scion phenotypes and patterns of phenomic covariation are highly dynamic across the season.</p> <p>Conclusions: These findings substantially expand previously identified patterns to demonstrate that rootstock influence on scion phenotypes is complex and dynamic and underscore that broad understanding necessitates volumes of multi-dimensional data previously unmet.</p>	
<b>Corresponding Author:</b>	Zachary N Harris Saint Louis University SAINT LOUIS, MO UNITED STATES	
<b>Corresponding Author Secondary Information:</b>		
<b>Corresponding Author's Institution:</b>	Saint Louis University	
<b>Corresponding Author's Secondary Institution:</b>		
<b>First Author:</b>	Zachary N Harris	
<b>First Author Secondary Information:</b>		
<b>Order of Authors:</b>	Zachary N Harris	
	Mani Awale	
	Niyati Bhakta	
	Daniel H. Chitwood	
	Anne Fennell	
	Emma Frawley	
	Laura L. Klein	

	Laszlo G. Kovacs
	Misha Kwasniewski
	Jason P. Londo
	Qin Ma
	Zoë Migicovsky
	Joel F. Swift
	Allison J. Miller
<b>Order of Authors Secondary Information:</b>	
<b>Response to Reviewers:</b>	<p>Note to all: Microsoft Word on macOS does not allow correct continuous line numbering with "track changes" on. All referenced line numbers were identified such that they were continuous. If line numbers appear way off, try changing "All Markup" to "Simple Markup" under the Review tab to align the line numbers.</p> <p>All revisions from this round are labelled Revision_2.</p> <p>Editor Comments:  With regards to Reviewer #4 comments and Github - if the manuscript is deemed acceptable for publication, GigaScience will always take snapshots and host that, along with other supporting data and metadata under a CC0 license. So despite the reviewer's concern about GitHub not being a permanent repository, there will be copies permanent in our open repository, GigaDB.  Response: We thank the editor for their work on this manuscript. We are happy to have additional copies of all of our scripts and data sets hosted redundantly across multiple repositories. Our intention with GitHub was to store the analysis scripts as permanent versions of record. As we do not come from software development, we were using GitHub as a convenient home rather than as a live repository for ongoing projects. One additional note: we uploaded all metabolomics data to Metabolites, but have not received a response from that submission. We would be happy to store an additional copy on GigaDB, if appropriate.</p> <p>Reviewer 1:  Relevant methodological information that was missing from the previous submission has been added to the revised manuscript by Harris and co-workers, which enables a more conscious interpretation of the results. Experimental limitations and external sources of variation have also been considered when discussing the results. In addition, cross-check of expected expression profiles for a selection of genes has been included as a validation of the RNA-seq experiment reliability.  Response: We thank the reviewer for their careful review and re-review of the manuscript. Comments made by reviewers have considerably strengthened the manuscript and we really appreciate it.</p> <p>Considering all the information, despite a huge multilevel dataset was generated, its value is limited by experimental design deficiencies recognized by the authors (e.g.: only one year of study under field conditions, noise of environmental/circadian variation during extensive physiological phenotyping and RNA-seq sampling throughout relatively long periods of the day, theoretically low power of the RNA-seq experiment due to relatively low read depth and low replication in some comparisons with only two replicates). Altogether, the manuscript is mostly descriptive of general differences rather than conclusive. Some of the main observations have already been documented before, such as the idea that rootstock genotype affects scion leaf phenotypes. Regardless, in the current version of the manuscript, the study and its limitations are fairly presented by the authors in a manner that would be acceptable for publication if the journal considers the dataset of value in spite of these experimental limitations. Besides this general concern, I would only have a few minor comments to this version:</p> <p>1. The dataset might still be undermined as only general descriptive differences are presented as conclusions, but nothing about their possible origin is mentioned. For instance, what are the known intrinsic features of the compared rootstocks according to the bibliography that could determine the observed differences in ionic composition?</p>

How could these rootstock-determined differences in ion accumulation affect vine performance? Similar questions would arise for other differences observed.  
-Response: Thank you for this comment, and we share a strong interest in understanding intrinsic features of rootstocks that affect the observed differences in the grafted scion. Studies that begin to get at these questions are underway within our research team now, but unfortunately are not completed and not included in this manuscript. To address the reviewer comments here, we specified that, especially in the case of the ionome, the differences are likely due to the genetics/ pedigree of the rootstock on L521-523. Additional comments added in the last round of revision explain how we are presently unsure how individual ions map to aspects of vine performance. We know even less about the other phenotypes. Future analyses using the data set we presented, additional data that were beyond the scope of leaf phenotyping, and future data can and should address this type of question.

2. It could be more specifically pointed out that lack of DEGs in some RNA-seq comparisons could be due to the experimental limitations (e.g.: low replication and 4.1 M read depth below the minimum recommended 5 M) rather than to a real lack of effect of rootstock genotype.

-Response: Agreed. We added a note to the Data Description that we opted to sequence more samples at the cost of some read depth which does limit our power to detect some low-expression genes on L195-196. We recognize that replication is low for high order interactions (rootstock:row:phenology) due to only sampling two vines per cell. Because of this low replication, we did not interpret such effects because they would be underpowered. However we sampled 36 cells at each time point for a total of 216 samples (with a few removed for poor sequencing), so lower order interactions and main effects were derived from much larger pools of clonally replicated samples. Specific details on this can be found in response to Reviewer 2 and 4 in the first revision.

3. The value of including PC covariation networks would be scarce if the results are not reliable enough for interpreting the inter-connection identified between the responsible specific metabolites, ions, genes, etc.

-Response: It's true, and we agree that any issues present in individual data sets will percolate into integrative analyses. Having said that, we are confident in the individual datasets and in our approach using those datasets in PC covariation networks. Focusing on PCs from each modality allowed us to capture the highest levels of variation to see how those PCs relate across modalities. We chose this analysis so that no particular modality was over-weighted and so that we could narrow down where interesting correlations lie such that we can design and craft better future studies. We recognize this approach has limitations, but after exploring many different potential options we felt this was the most appropriate given the data and the questions.

4. Several typos should be corrected in the newly added text.

-Response: We thank the reviewer for the close reading of the text. We have edited the manuscript for typos, grammar, and tense.

Reviewer 2:

I was pleased to review the resubmitted manuscript by Harris and co-workers, who have responded to my original review. The Authors have clarified a number of points regarding the RNAseq experiments including RNA extraction methods, and the tissue type that was used. More information has been added to the methods that would aid reproducibility. Additional statistics have been applied to Figures 1 and 5. Numerous formatting and grammatical changes have been made that improve the readability of the manuscript. Additional supporting references have been provided. While not all of my suggestions were included, I accept the authors responses to my original review. I have no further concerns and recommend the manuscript for publication in GigaScience.

-Response: We thank the reviewer for their careful considerations of our manuscript. The manuscript has been considerably improved thanks to the reviewer's comments.

Reviewer 3:

I found that the Authors clearly improved the ms which might be suitable for publication

-Response: We thank the reviewer for their careful considerations of our manuscript.

	<p>We especially thank the reviewer for comments on improving figures. The presentation of our work was improved by the reviewer's comments.</p> <p>Reviewer 4:  -I saw the editor comments about appropriate data storage, but I disagree with those comments to the authors.  -Github is not a permanent repository and as such it's not true that it's the most appropriate place to share scripts for a publication. It is only suitable as a place for collaboration. As the authors make changes, the version of record for this manuscript will no longer be available, and the authors could delete it at any time. The publication versions should be separately repositied in a permanent repository. In my opinion, if a script is meant to be a version of record and also living, then a link to both the permanent repository and to GitHub can be given.  -I am not sure what is meant by 'large-scale' data. Figshare is a general use repository that I only recommended since the authors already were using it. It can host single files up to 5 gb in size, provides unlimited public space, and provides a DOI. So what exactly is unsuitable?  -Zenodo is another free option, and there is Data Dryad and the Data Commons.</p> <p>-Response: We thank the reviewer for their careful considerations of our manuscript. We are happy to share our data and scripts in any way requested. Our intention was to use Github as a repository for a version of record, but we recognize that it is not a perfect solution. We are happy that Gigascience will host snapshots so that there is no potential for misuse. If the reviewer would like an additional home for the scripts we would be very happy to do that.</p>
<b>Additional Information:</b>	
<b>Question</b>	<b>Response</b>
Are you submitting this manuscript to a special series or article collection?	No
<p><b>Experimental design and statistics</b></p> <p>Full details of the experimental design and statistical methods used should be given in the Methods section, as detailed in our <a href="#">Minimum Standards Reporting Checklist</a>. Information essential to interpreting the data presented should be made available in the figure legends.</p> <p>Have you included all the information requested in your manuscript?</p>	Yes
<p><b>Resources</b></p> <p>A description of all resources used, including antibodies, cell lines, animals and software tools, with enough information to allow them to be uniquely identified, should be included in the Methods section. Authors are strongly encouraged to cite <a href="#">Research Resource Identifiers</a> (RRIDs) for antibodies, model</p>	Yes



<p>organisms and tools, where possible.</p> <p>Have you included the information requested as detailed in our <a href="#">Minimum Standards Reporting Checklist</a>?</p>	
<p><b>Availability of data and materials</b></p> <p>All datasets and code on which the conclusions of the paper rely must be either included in your submission or deposited in <a href="#">publicly available repositories</a> (where available and ethically appropriate), referencing such data using a unique identifier in the references and in the “Availability of Data and Materials” section of your manuscript.</p> <p>Have you have met the above requirement as detailed in our <a href="#">Minimum Standards Reporting Checklist</a>?</p>	Yes



# 1 **Multi-dimensional leaf phenotypes reflect root system genotype in grafted** 2 **grapevine over the growing season**

3  
4 Zachary N. Harris<sup>1,2\*</sup> (zachary.n.harris@slu.edu), Mani Awale<sup>3</sup> (maybd@mail.missouri.edu), Niyati  
5 Bhakta<sup>1,2</sup> (niyatisbhakta@gmail.com), Daniel H. Chitwood<sup>4,5</sup> (chitwoo9@msu.edu), Anne Fennell<sup>6</sup>  
6 (anne.fennell@sdstate.edu), Emma Frawley<sup>1,2</sup> (emma.frawley@wustl.edu), Laura L. Klein<sup>1,2</sup>  
7 (laura@leafworks.com), Laszlo G. Kovacs<sup>7</sup> (laszlokovacs@missouristate.edu), Misha Kwasniewski<sup>3</sup>  
8 (mtk5407@psu.edu), Jason P. Londo<sup>8</sup> (jason.londo@usda.gov), Qin Ma<sup>9</sup> (qin.ma@osumc.edu), Zoë  
9 Migicovsky<sup>10</sup> (zoe.migicovsky@dal.ca), Joel F. Swift<sup>1,2</sup> (joel.swift@slu.edu), and Allison J. Miller<sup>1,2\*</sup>  
10 (allison.j.miller@slu.edu)

11  
12 <sup>1</sup>Department of Biology, Saint Louis University, 3507 Laclede Avenue, St. Louis, MO, 63103-2010, USA

13 <sup>2</sup>Donald Danforth Plant Science Center, 975 North Warson Road, St. Louis, MO, 63132-2918, USA

14 <sup>3</sup>Division of Plant Sciences, University of Missouri, 135 Eckles Hall, Columbia, MO, 65211, USA

15 <sup>4</sup>Department of Horticulture, Michigan State University, East Lansing, MI, 48824, USA

16 <sup>5</sup>Department of Computational Mathematics, Science and Engineering, Michigan State University, East  
17 Lansing, MI, 48824, USA

18 <sup>6</sup>Department of Agronomy, Horticulture & Plant Science, South Dakota State University, Brookings, SD,  
19 57006, USA

20 <sup>7</sup>Department of Biology, Missouri State University, 901S. National Avenue, Springfield, MO, 65897,  
21 USA

22 <sup>8</sup>United States Department of Agriculture, Agricultural Research Service: Grape Genetics Research Unit,  
23 630 West North Street, Geneva, NY, 14456-1371, USA

24 <sup>9</sup>Department of Biomedical Informatics, The Ohio State University, 1585 Neil Ave, Columbus, OH,  
25 43210

26 <sup>10</sup>Department of Plant, Food, and Environmental Sciences, Faculty of Agriculture, Dalhousie University,  
27 Truro, NS, B2N 5E3, Canada

28 \* To whom correspondence should be addressed

29  
30  
31  
32  
33  
34  
35

Formatted: Normal

Style Definition: Heading 1

Style Definition: Heading 2

## 36 **Abstract**

37 Background: Modern biological approaches generate volumes of multi-dimensional data, offering  
38 unprecedented opportunities to address biological questions previously beyond reach due to small or  
39 subtle effects. A fundamental question in plant biology is the extent to which below-ground activity in the  
40 root system influences above-ground phenotypes expressed in the shoot system. Grafting, an ancient  
41 horticultural practice that fuses the root system of one individual (the rootstock) with the shoot system of  
42 a second, genetically distinct individual (the scion), is a powerful experimental system to understand  
43 below-ground effects on above-ground phenotypes. Previous studies on grafted grapevines have detected  
44 rootstock influence on scion phenotypes including physiology and berry chemistry. However, the extent  
45 of the rootstock's influence on leaves, the photosynthetic engines of the vine, and how those effects  
46 change over the course of a growing season, are still largely unknown.

47 Results: Here, we investigate associations between rootstock genotype and shoot system phenotypes  
48 using five multi-dimensional leaf phenotyping modalities measured in a common grafted scion: ionomics,  
49 metabolomics, transcriptomics, morphometrics, and physiology. Rootstock influence is ubiquitous but  
50 subtle across modalities with the strongest signature of rootstock observed in the leaf ionome. Moreover,  
51 we find that the extent of rootstock influence on scion phenotypes and patterns of phenomic covariation  
52 are highly dynamic across the season.

53 Conclusions: These findings substantially expand previously identified patterns to demonstrate that  
54 rootstock influence on scion phenotypes is complex and dynamic and underscore that broad  
55 understanding necessitates volumes of multi-dimensional data previously unmet.

56

## 57 **Background**

58

59 High-throughput data acquisition has afforded unprecedented capacity to quantify and understand  
60 plant form and function. Recent advances in imaging and computation have expanded our ability to  
61 measure plant traits or phenotypes [1,2], and to extend those comprehensive measurements into

62 latent space phenotypes ~~{3}~~[3]. Now broadly known as phenomics, this burgeoning field is characterized  
63 as the acquisition and analysis of high-dimensional phenotypic data at different hierarchical levels  
64 ~~{4,5}~~[4,5], often with an eye toward multiscale data integration. A holistic and hierarchical approach to  
65 plant phenotypic variation affords unique insights into plant evolution and how plants change over  
66 development and in response to environmental cues and horticultural manipulation.

67 A fundamental question in plant biology is how root systems influence phenomic variation in  
68 above-ground shoot systems including leaves, flowers, and fruits. Grafting, a common horticultural  
69 manipulation that joins the shoot system of one individual (the scion) with the root system of another  
70 individual (the rootstock), is commonly used in crop species to confer favorable phenotypes to  
71 commercial scions ~~{6}~~[6], including enhanced disease resistance ~~{7,8}~~[7,8], fruit quality, plant form ~~{9}~~[9],  
72 response to water stress ~~{10}~~[10], and growth on particular soils ~~{11,12}~~[11,12]. Because grafting often  
73 uses clonally propagated materials, it is possible to manipulate and replicate different combinations of  
74 root systems and shoot systems, offering a valuable experimental system in which root system impacts on  
75 shoot system phenotypes can be evaluated.

76 The European grapevine (*Vitis vinifera*) is among the most economically important grafted crops  
77 in the world. Grapevines are cultivated primarily for fruits used to make wine and juice, as well as for  
78 table grape and raisin production. Grafting in grapevines became widespread in the mid-1800's following  
79 the accidental introduction of the root-feeding aphid phylloxera from its native North America into  
80 Europe, where it began attacking the roots of European grapevines ~~{13}~~[13]. Because European  
81 grapevines often do not survive phylloxera infestation, in regions where phylloxera has been introduced  
82 most grapevine cultivation consists of European grapevines grafted to rootstocks derived from  
83 phylloxera-resistant North American *Vitis* species including *V. berlandieri*, *V. riparia*, and *V. rupestris*,  
84 and their hybrid derivatives. In addition to grapevines, more than 70 major perennial crops are grafted  
85 including many fruit trees and vines ~~{9}~~[9]. Grafting decouples the breeding of shoot systems and root  
86 systems, with selection in plants targeted for use as scions focusing primarily on fruit phenotypes, and

87 selection in plants targeted for use as rootstocks focused on below-ground biotic and abiotic stress  
88 resistance, as well as their impacts on shoot system phenotypes.

89         The effects of grafting in grapevine show a remarkable breadth of scion response patterns. For  
90 example, a study of *Vitis vinifera* cv. ‘Cabernet Sauvignon’ grafted to different rootstocks identified  
91 transcriptome reprogramming in the scion of grafted plants; this appeared to be a general effect of  
92 grafting to a rootstock and was not rootstock-specific [14],[14]. In contrast, other studies have found  
93 signatures of rootstock genotype in the transcriptome in early berry development, although this distinction  
94 was lost in later development [15,16], but see [17],[15,16], but see [17]. Comprehensive phenomic  
95 analyses, including those that link transcriptome data with other high-throughput phenotyping assays,  
96 offer an opportunity to expand understanding of rootstock effects on grapevine shoots. In one study,  
97 leaves of the *V. vinifera* cultivar ‘Gaglioppo’ showed variation in stilbene and abscisic acid  
98 concentrations due to rootstock genotype, as well as differences in transcriptional profiles [18],[18].  
99 Likewise, gene expression, ion concentrations, and leaf shape in the cultivar ‘Chambourcin’ varied in  
100 response to rootstock genotype [18,19],[18,19]. Collectively, these studies suggest the impacts of grafting  
101 are diverse and may vary over the course of vine development. However, to date few studies have  
102 surveyed multiple high-dimensional scion phenotypes to understand rootstock influence on shoot system  
103 phenotypes over the course of the growing season or the extent to which grafting effects on the scion  
104 covary with one another.

105         Leaves are the photosynthetic engine of the organism and a primary site for perception and  
106 response to environmental change. Grapevine leaves have been used for centuries as markers of species  
107 and cultivar delimitation, developmental variation, disease presence, and nutrient deficiency  
108 [20,21],[20,21]. More recently, analysis of grapevine leaf morphology has identified genetic architecture  
109 of leaf shapes [22],[22], developmental patterns across the season [23],[23], and signatures of evolution in  
110 the grapevine genus [24],[24]. Grapevine leaves respond to stress through gas and water exchange with  
111 the atmosphere [25,26],[25,26] and have been shown to differentially partition the ionome depending on  
112 their position on the shoot [19],[19] and their rootstock genotype [19,27,28],[19,27,28]. The volume of

113 work on grapevine leaves provides a foundation for the analysis of phenomic variation in a vineyard over  
114 a season in response to grafting.

115 In this study, we investigate effects of grafting on high dimensional leaf phenotypes of the hybrid  
116 cultivar ‘Chambourcin’ over the course of the growing season. We quantify leaf elemental (ion)  
117 concentrations, metabolite abundance, gene expression, shape, and vine physiology in a replicated  
118 rootstock trial where the hybrid grapevine cultivar ‘Chambourcin’ is growing ungrafted and grafted to  
119 three different rootstocks. The four root-shoot combinations (‘Chambourcin’ ungrafted, ‘Chambourcin’  
120 grafted to three different rootstocks) are replicated 72 times in a randomized block experimental design  
121 with an irrigation treatment (Supplemental Figure 1). Phenotypic data, data that describe variation for a  
122 particular trait within a particular modality, were collected either on the full 288-vine set (ion  
123 concentrations, leaf shape) or on a subset of 72 vines (the 72-vine set; metabolite abundance, gene  
124 expression, vine physiology). Using data collected at three time points that span the growing season  
125 (anthesis, veraison, and harvest), we show that all phenotyping modalities (ionomic, metabolomic,  
126 transcriptomic, morphometric, and physiology phenotypes) reflect subtle but ubiquitous responses to  
127 grafting and rootstock genotype. Rootstock effects on shoot system phenotypes were often dynamic  
128 across the season, suggesting that accounting for seasonal variation could enhance our understanding of  
129 grafting effects in viticulture.

130

## 131 **Data Description**

132

### 133 *Leaf Ionomics*

134 The ionome describes elemental composition of a tissue at a particular time point ~~[29]~~[29]. Three  
135 leaves per vine were collected from the 288-vine set at three seasonal time points: anthesis (~mid May),  
136 veraison (~late July), and harvest ~mid September). Leaves were sampled from a single shoot and  
137 included the youngest fully opened leaf at the shoot tip, the approximate middle leaf, and the oldest leaf at  
138 the shoot base. Teams were deployed in the vineyard so that multiple vineyard rows were being sampled



139 concurrently. As such, 'block' represented unmeasured spatial variation, but did not strictly correlate with  
140 time of sampling due to the nature of sampling (see Methods). Whole leaves were placed in zip-lock bags  
141 in the field and stored in a cooler on ice packs, scanned for leaf shape analysis in the lab (see Leaf Shape)  
142 and then dried in coin envelopes at 50°C for one to three days for elemental analysis. Between 20 and 100  
143 mg of leaf tissue was acid digested and 20 ions were quantified using inductively coupled plasma mass  
144 spectrometry (ICP-MS) following standard protocol of the Donald Danforth Plant Science Center  
145 (DDPSC) Ionomics Pipeline ~~[30,31]~~[30,31]. Ion quantifications were corrected for internal standard  
146 concentrations, instrument drift and by initial sample mass. The output of the Pipeline contained  
147 estimated concentrations of each of the following 20 elements: Al, As, B, Ca, Cd, Co, Cu, Fe, K, Mg, Mn,  
148 Mo, Na, Ni, P, Rb, S, Se, Sr, and Zn. For each ion concentration, we computed z-score distributions and  
149 used those values as the basis for linear models. Following convention, non-standardized values were  
150 used for machine learning analysis.

151

### 152 *Leaf Metabolomics*

153 The metabolome comprises small mostly organic molecules present in a tissue and represents a  
154 catalogue of the products of metabolic processes ~~[32,33]~~[32,33]. Metabolomic analysis was completed at  
155 veraison (the onset of fruit ripening) and immediately prior to harvest for the 72-vine set. For each vine,  
156 three mature leaves were sampled from the middle of a single shoot and immediately flash frozen in  
157 liquid nitrogen in the field to capture the metabolic state of the leaves when attached to the vine. Leaves  
158 were sampled by a single team near midday in row and block order, ensuring that 'block' captured both  
159 unmeasured spatial variation and temporal variation over the sampling window (see Methods). Frozen  
160 leaves were transported to the University of Missouri Enology Lab on dry ice and stored at -80°C.  
161 Following the protocol of [34][34], whole leaves were manually ground in liquid nitrogen with a mortar  
162 and pestle, 0.5g of powder was weighed into a centrifuge tube, 1.5ml of 1:1 MeOH: ACN was added.  
163 Samples were vortexed to suspend leaf particles and sonicated for 20 minutes in an ice bath. After

164 extraction, samples were centrifuged for 10 minutes at 3,000 g and filtered with a 0.22 PTFE syringe filter  
165 into a 1.5ml sample vial before injecting into a Waters XEVOTM QToF LCMS system (Waters  
166 Corporation, Milford, MA, USA). Chromatographic separation was achieved using a Waters Acquity TM  
167 Ultra Performance LC H-Class system (Waters Corporation, Milford, MA, USA) equipped with Waters  
168 Acquity BEH C18 column (2.1mmx150mm and 1.7um particle size) and a diode array detector. Samples  
169 were injected in random order across the sampling periods. The injection volume was set at 2.5ul and the  
170 flow rate was set at 0.4 ml/min. The mobile phase consisted of 0.1% formic acid in water (solvent A) and  
171 0.1% formic acid and 5% water in acetaldehyde (solvent B) and the gradient was as follows: 100% A for  
172 0.5 min; 0.5-18min increased to 99% B; 18-19 min. held at 99% B; mobile phase was re-equilibrated for  
173 2 min between runs. Diode array was monitored at 225-500nm. Mass spectrometry was performed on a  
174 XevoTM QToF (Waters Corporation, Milford, MA, USA). The electrospray ionization (ESI) was operated  
175 in both positive or negative ionization modes in separate runs. The scan range was set as m/z 50-1500  
176 with 0.2 sec accumulation time. MS settings were as follows: capillary voltage was 2.5kV; cone voltage  
177 ramped from 20-40V; collision energy was set to 6V; detector voltage was set to 1950V; desolvation gas  
178 was set to 1000 L/hour; cone gas was set to 50 L/hr; source temperature was 120 °C and desolvation  
179 temperature was set at 550 °C.

180 LC-MS instrument files were converted to .cdf format and uploaded to XCMS online [\[35\]\[35\]](#) for  
181 chromatogram normalization and feature detection via “single job” parameters. The 661 identified  
182 metabolomic features were used as the basis of a principal components (PC) analysis. The top 20 PCs  
183 were treated as distinct phenotypes to model according to the experimental design. In PCs that varied  
184 significantly by rootstock, features that loaded more than 1.96 standard deviations above or below the  
185 mean were fit independently with the same model design.

#### 186 *Leaf Gene Expression*

187 The youngest fully-opened leaves on two shoots were collected from each plant of the 72-vine set  
188 (see Study Design). The two leaves, which were distinct from leaves used for ionomics, leaf shape,

189 metabolomics and physiology data collection, were pooled for RNA sequencing. Leaves were sampled by  
190 a single team near midday between 10AM and 2PM in row order, ensuring that ‘block’ and ‘row’  
191 accounted for unmeasured spatial variation and temporal variation over the sampling window (see  
192 Methods). Samples were sequenced using 3’-RNAseq, a method ideal for organisms with reasonably  
193 characterized reference genomes [36],[36]. Total RNA was extracted from plant tissues using the Sigma  
194 Spectrum Plant Total RNA kit with modification of the addition of 2% PVP40 to the extraction buffer to  
195 decrease phenolic inhibitors. All RNA extractions were checked for quality control using a Nanodrop.  
196 Sequencing was conducted using the Illumina NextSeq500 platform which returned single-end 86 bp  
197 reads. To accommodate the large number of samples in this study, we opted to obtain fewer reads per  
198 sample, which might have limited our ability to detect differential expression in lowly-expressed genes.  
199 The first 12 nucleotides from each read were trimmed to remove low-quality sequences using  
200 Trimmomatic (options: HEADCROP:12; [37],[37]). Low quality trimmed reads were additionally  
201 identified based on overrepresentation of kmers and removed using BBduk (April 2019 release) [38],[38].  
202 Trimmed and QC-controlled reads were mapped to the 12Xv2 reference *Vitis vinifera* genome  
203 [39,40][39,40] using STAR (v2.7.2b) [41],[41] with default alignment parameters. RNAseq read  
204 alignments were quantified using HTSeq-count (v0.11.2) [42],[42] and a modified version of the VCost.v3  
205 reference *V. vinifera* genome annotation [40],[40]. To capture mis-annotated gene body boundaries in the  
206 genome, all gene boundaries in the annotation were extended 500 bp.

207 Variation in gene expression was assessed using two methodologies. First, we identified  
208 individual genes which responded to specific factors in the experimental design using DESeq2 (v1.24.0)  
209 [43],[43]. Each gene was fit with the model “~ Block + Irrigation + Phenology\_Rootstock” where the  
210 ‘Phenology\_Rootstock’ model term was used to understand the potential interaction of phenology and  
211 rootstock. Genes were filtered to a gene set that included only genes with a normalized count greater than  
212 or equal to two in at least five samples. To check the validity of our expression results, we assayed two  
213 classes of housekeeping genegenes (Ubiquitin-domain and actin-family) and eight previously annotated  
214 circadian genes [44],[44] (Supplemental Figure 2). Differentially expressed genes were identified for each

215 pairwise contrast in the model. Second, we used principal component analysis (PCA) to collapse variation  
216 in co-expressed genes into fewer dimensions. Normalized count-filtered genes from DESeq2 were  
217 transformed using the variance stabilizing transformation (VST; ~~f45~~[45]) and input into a PCA. We then  
218 analyzed the top 100 PCs in the context of the broader experimental design. We previously showed that  
219 the transcriptome varied by the time of collection and was potentially interacting with the rootstock effect  
220 ~~f19~~[19]. Moreover, the other modalities in this study point to weak if any effects from the irrigation  
221 treatment (see Supplemental Note 1). Due to the nature of the vineyard design, we could not identify both  
222 irrigation and time effects (marked by row) in a single model (irrigation and row are collinear; see Study  
223 Design). To approximate the impact from time of collection (row) in the vineyard on gene expression,  
224 linear models were first fit to remove variation imparted by irrigation from each of the top 100 PCs. The  
225 residuals were then used as the basis for linear models and machine learning analysis.

226

### 227 *Leaf Shape*

228 All leaves from a single shoot directly emerging from a trained cordon were collected from each  
229 vine in the 288-vine set at anthesis and veraison. At harvest, we collected only the oldest (first emerging  
230 leaf), middle (estimated from the middle of a whole shoot), and youngest (smallest fully emerged leaf at  
231 the shoot tip, >1cm). Leaves were collected approximately in row order (from south to north) and stored  
232 in a cooler. Each leaf was imaged using an Epson DS-50000 scanner in color against a white background  
233 at 1200 DPI and written as JPEG formatted images. Following scanning of leaves for leaf shape analysis,  
234 the oldest, middle, and youngest leaves were dried and used to estimate leaf elemental composition (see  
235 Ionomics). As the leaf shape samples and ionomics samples were identical, 'block' represented  
236 unmeasured spatial variation, but did not strictly correlate with time of sampling (see Methods). While all  
237 leaves were collected from a single shoot, only the oldest, middle, and youngest leaves were used in this  
238 analysis.

239 We assessed leaf shape using Generalized Procrustes Analysis (GPA) of landmarks. For the three  
240 leaves per vine used in leaf shape analysis, 17 homologous landmark features were identified ~~f22~~[22].

241 The GPA-rotated coordinate space was used for all subsequent statistical analysis including PCA in order  
242 to summarize variation in leaf shape ~~[46],[46]~~. From the PCA, we extracted the top 20 PCs and fit linear  
243 models and machine learning models to describe variation.

#### 245 *Vine physiology*

246 Intracellular CO<sub>2</sub> concentration, stomatal conductance and leaf transpiration rate were measured  
247 at midday (each measured simultaneously between 10am to 1pm) on one fully expanded sun-exposed leaf  
248 for each of the vines in the 72-vine set. Physiology measurements were taken in row order ensuring that  
249 'block' correlated with temporal variation over the sampling window. Measurements were taken using an  
250 LI-6400XT Portable Photosynthesis system coupled with a pulse amplitude-modulated (PAM) leaf  
251 chamber fluorometer (Li-Cor, Inc., Lincoln, NE, USA) with the following parameters: incident  
252 photosynthetic photo flux density level of 1000  $\mu\text{mol m}^{-2} \text{s}^{-1}$  generated by a red LED array and 10%  
253 blue light to maximize stomatal opening, CO<sub>2</sub> mixer of 400  $\mu\text{mol/s}$ , fixed flow of 300  $\mu\text{mol/s}$ , and  
254 ambient leaf and block temperature. Soil moisture was measured for each plant in the 72-vine set using a  
255 fieldScout TDR 300 Moisture meter equipped with 20 cm rods (Spectrum Technologies, Inc. Aurora, IL,  
256 USA). Midday stem water potential was measured using a pressure bomb/chamber (PMS Instrument Co.,  
257 Albany, OR, USA) after enclosing the leaves in an aluminum foil bag for at least 15 minutes to  
258 equilibrate the water potential of the xylem in the stem to that attached leaf (for a discussion on  
259 equilibration time, see ~~[47,48]],[47,48]~~).

#### 261 **Analyses**

##### 263 *Leaf ionome*

264 To characterize the leaf ionome over the growing season, we sampled the youngest, middle, and  
265 oldest leaf from a single shoot from each of the vines within the 288-vine set at three phenological stages

Formatted: Normal

Formatted: Font: Cardo

266 and measured the concentrations of 20 ions in each leaf individually. Bivariate correlations showed that  
267 ion concentrations are not independent of each other, but that the strength and direction of relationships  
268 between ions vary with respect to phenological stage and leaf position (Supplemental Figure 3). As such,  
269 we fit independent linear models to each ion. Leaf position, phenological stage, or the interaction of  
270 phenological stage and leaf position explained the highest amount of variation for most ions (Figure 1A-  
271 B). Many ions significant for the interaction showed a clear signal of leaf position at anthesis and  
272 veraison, and either no explainable variation or muted variation at harvest. For example, calcium (Figure  
273 1B) varied with leaf position (22.7% variation explained;  $p < 1e-05$ ), phenology (24.0%;  $p < 1e-05$ ), and  
274 their interaction (7.4%,  $p < 1e-05$ ). All possible pairwise combinations of leaf position were significantly  
275 different at anthesis, and both the youngest and middle leaves were different from the oldest leaves at  
276 veraison and harvest. In the case of potassium (Figure 1B), significant variation was explained by leaf  
277 position (16.1%;  $p < 1e-05$ ), phenology (19.6%;  $p < 1e-05$ ), and their interaction (10.6%;  $p < 1e-05$ ).  
278 However, post-hoc comparisons of phenology-wise mean calcium concentrations showed that differences  
279 were present only at anthesis and veraison.

280 Rootstock genotype showed remarkable influence on the composition of the leaf ionome. All ions  
281 except aluminum, sodium, and zinc were significant for rootstock as a single fixed effect (Figure 1A).  
282 Rootstock explained between 0.4% (rubidium;  $p = 3.2e-05$ ) and 14.3% (nickel;  $p < 1e-05$ ) of variation ion  
283 concentrations (Figure 1A). For some ion concentrations (such as cobalt and nickel), significant variation  
284 was explained by the interaction of rootstock and phenology; this pattern was observed mostly in ions that  
285 responded weakly to the interaction of leaf position and phenology. These ions showed similar patterns to  
286 the leaf position by phenology interaction where a clear signal was exhibited at anthesis and veraison then  
287 ~~is~~was either absent or muted at harvest. For example, cobalt was most abundant in '1103P'-grafted vines  
288 at anthesis (Figure 1C). At veraison, both '1103P'-grafted and 'SO4'-grafted had elevated concentrations  
289 compared to Ungrafted and '3309'-grafted vines. However, by harvest, cobalt concentration variation was  
290 muted and only 'SO4'-grafted vines showed evidence of elevated concentration. Similarly, nickel showed  
291 significant variation partitioned into the rootstock by the phenology effect (Figure 1C). Both anthesis and



292 veraison show reduced nickel concentration in '1103P'-grafted vines and elevated concentrations in  
293 'SO4'-grafted vines. However, at harvest, no comparisons are significant.

294 Machine learning on ion concentrations confirms that the leaf ionome contains a signature from  
295 the rootstock genotype and the interactions of rootstock genotype with phenology and leaf position. A  
296 random forest model trained to predict rootstock showed an overall accuracy of 75.2% (Figure 1D). Ions  
297 important for this classification were nickel (Mean Decrease in Accuracy (MDA)=0.089), molybdenum  
298 (MDA=0.058), and magnesium (MDA=0.054), corroborating the rootstock term's significance in the  
299 linear models. Notably, when we trained a model to simultaneously predict rootstock and phenological  
300 stage, rootstock prediction accuracy increased appreciably (Figure 1E). For example, the ability of the  
301 model to detect ungrafted vines (the balanced accuracy of ungrafted predictions) improved from 81.7%  
302 accuracy overall to 91.1% accuracy at anthesis and 85.9% at harvest. Generally, performance at veraison  
303 matched the rootstock-only model performance. The ions most important for this joint  
304 (rootstock/phenological stage) prediction were nickel (MDA=0.167), phosphorus (MDA=0.110), and  
305 strontium (MDA=0.065). The rootstock by phenology model term was significant in the linear models for  
306 these ions, but was not a largest descriptor of variation. The joint prediction of rootstock and leaf position  
307 performed substantially better than chance ( $p < 1e-05$ ), but accounting for leaf position did not improve  
308 rootstock prediction as was the case in the joint prediction of rootstock and phenology (Figure 1F). Ions  
309 important for this classification were sulfur (MDA = 0.051), rubidium (MDA = 0.051), and nickel (MDA  
310 = 0.049).

311

### 312 *Leaf metabolomics*

313 We performed untargeted metabolomics on leaves from the 72-vine set at veraison and harvest,  
314 quantifying the concentrations of 661 metabolites (Figure 2). The top 20 PCs accounted for a total of  
315 67.3% of the total metabolomic variation, with the top three capturing 23.1%, 9.2%, and 6.2%,  
316 respectively. Individual PCs after the top 20 explained less than 0.82% of the metabolome. Linear models  
317 for each of the top 20 PCs found that the strongest drivers of variation in leaf metabolomics were

318 phenology and temporal blocking factor. For example, 90.6% of variation on PC1 was due to phenology  
319 ( $p < 1e-05$ ; Figure 2A). PC2 primarily reflected the interaction of phenology and temporal block (26.4%,  
320  $p < 1e-05$ ) and temporal block as a main effect (18.9%,  $p < 1e-05$ ). The patterns of variation attributable  
321 to PC2 were similar in PCs 3-10 (Figure 2A).

322 PC17 was controlled by rootstock as a main effect (18.5%,  $p < 1e-03$ ; Figure 2B). On PC17,  
323 ungrafted vines were significantly different from vines grafted to '3309C' ( $p = 0.02$ ) and 'SO4' ( $p < 1e-$   
324  $05$ ). Vines grafted to '1103P' were also significantly different from vines grafted to 'SO4' ( $p = 0.009$ ).  
325 Metabolites that loaded more than 1.96 sd from the mean loading on PC17 were extracted and  
326 independently fit to additional linear models. We identified four metabolite features (M374T1 [rt = 1.33,  
327  $m/z = 374.1146$ ], M117T1 [rt = 0.61,  $m/z = 117.0583$ ], M175T1\_1 [rt = 0.87,  $m/z = 175.1269$ ], and  
328 M333T1\_3 [rt = 0.71;  $m/z = 333.1582$ ]) which were influenced by rootstock as a main effect and the  
329 metabolite (M112T1 [rt = 1.48,  $m/z = 112.0061$ ]) which was influenced by the interaction of rootstock  
330 genotype and phenological stage. At this time, the identification of these features remains unknown.

331 Linear discriminant analysis confirmed that many experimental factors likely influence the  
332 metabolome. For example, when trained to maximize variation between classes of rootstocks, the model  
333 identified a space that weakly separates '1103P'-grafted and 'SO4'-grafted vines from ungrafted and  
334 '3309C'-grafted vines (LD1) and separates '3309C'-grafted vines from other classes (on LD2) (Figure  
335 2C). Despite this, machine learning showed minimal predictability for any class other than phenology,  
336 which was predictable with an accuracy of 100% for withheld samples. Rootstock genotype based on the  
337 metabolome was not predictable with accuracy only marginally better than chance (34.6%).

338

### 339 *Gene Expression*

340 We performed 3'-RNAseq on the youngest fully-opened leaves of the 72-vine set at three time  
341 points (Figure 3). On average, each sample contained 4.1 million 3'-reads and measured the expression of  
342 17,852 genes. Overall, we identified variation in 23,460 genes that had a DESeq2-normalized count  
343 greater than two in at least five samples. We computed the expression of two classes of housekeeping

344 genes, and showed that they are generally stable across samples over phenological time (Supplemental  
345 Figure 2). We noted that some variation is expected for housekeeping genes; see, for example, [49]-[49].  
346 Moreover, we showed that patterns of previously annotated circadian genes conform to expected results  
347 over the sampling window. For example, predicted orthologs of *LHY* and *RVE1* are correlated and  
348 decreasing over our sampling window, and a predicted *TOC1* ortholog is invariant. The results of these  
349 analyses provide general confidence in the gene expression data presented here.

350 Using a traditional differential expression analysis framework based on established DGE software  
351 (Deseq2), all genes returned as significantly differentially expressed by rootstock appeared to be false  
352 positives, evidenced by a single extreme outlier altering group means. Hierarchical clustering of the 500  
353 most variable genes after variance stabilizing transformation (VST) showed strong latent structure in the  
354 transcriptome and that most variation in the transcriptome was explained by the phenological stage  
355 (Figure 3A). The top 100 PCs on the VST-transformed gene counts accounted for nearly 92.3% of  
356 variation in the transcriptome. Linear models on each of the top 100 PCs indicated that 82.4% and 61.4%  
357 of the variation on PC1 and PC2 respectively were attributable to the phenological stage (Figure 3B-C).  
358 Row was also a significant descriptor of variation as a single, fixed effect and in interactions with  
359 rootstock and phenological stage. For example, row accounted for 36.0% and 43.3% of the variation on  
360 PC4 and PC6, respectively. Interacting with the phenological stage, row accounted for >10% of variation  
361 on 17 additional PCs.

362 Patterns of gene expression identified through LDA corresponded to phenological stage, vine  
363 row, and rootstock. LDA separated phenological stages into three distinct, non-overlapping groups in the  
364 space spanning LD1 and LD2 (Supplemental Figure 4). When trying to separate rows into distinct classes,  
365 the model converged on a 'horseshoe' shape in the LD1- LD2 space (Figure 3D), suggesting either a  
366 circadian topology to the transcriptome or continuous spatial variation over the vineyard [50]-[50]. LD1  
367 maximized the variation between row 8 (sampled early in the day) and row 16 (sampled a few hours  
368 later). LD2 maximized the separation of both rows 8 and 16 with row 12 (the row sampled in the middle  
369 of the sampling window). A model trained to separate rootstock classes (Figure 3E) showed that LD1

370 separated the rootstock 1103P from other rootstock genotypes, and LD2 primarily separated the rootstock  
371 '3309C' from ungrafted vines (Supplemental Figure 4).

372 Formal machine learning on gene expression PCs largely supported the linear models. A random  
373 forest trained to predict phenological stage classified testing samples with 92.9% accuracy. Anthesis was  
374 the most predictable class with a balanced accuracy of 100%; veraison and harvest displayed balanced  
375 accuracies of 92.7% and 92.4%, respectively. The PCs most important in phenology prediction were PC1  
376 (MDA = 0.16) and PC2 (MDA = 0.12). Gene expression PCs were unable to predict rootstock, with a  
377 total prediction accuracy of 23.4%. While no features were especially important in the prediction  
378 processes, PC44 showed the largest mean decrease in Gini impurity corroborating its signal in the linear  
379 models.

380

#### 381 *Leaf shape*

382 We collected leaves from the 288-vine set at three time points and landmarked a total of 2,422  
383 leaves (Figure 4). Homologous leaf landmarks were used for Generalized Procrustes Analysis (GPA).  
384 PCA on the GPA-rotated coordinates revealed ~97.2% of the total shape variation was captured by the  
385 top 20 principal components with PC1, PC2, and PC3 explaining 24.1%, 19.0%, and 13.3% of the  
386 variation respectively. Lower values on PC1 primarily capture leaves with shallow petiolar sinuses and  
387 short midvein distance from the depth of the superior sinus to the top of the midvein, whereas higher  
388 values on PC1 capture the opposite (Figure 4A). Similarly, lower values on PC2 capture deep petiolar  
389 sinuses combined with very shallow superior sinuses, and vice versa for higher values. PC3 primarily  
390 captures asymmetry (Figure 4A).

391 In total, 5.76% of variation on PC1 was explained by the experimental design. Of this, variation  
392 in leaf shape was explained by phenology (2.63%;  $p_{adj} < 1e-05$ ), then rootstock (0.95%;  $p_{adj} < 0.001$ ),  
393 leaf position (2.61%;  $p_{adj} = 0.03$ ), and the interaction of phenology and leaf position (0.62%;  $p_{adj} =$   
394 0.009) (Supplemental Figure 5A). Post-hoc mean comparisons on PC1 showed that shapes of leaves from  
395 ungrafted vines were significantly different from leaves of vines grafted to 1103P ( $p < 0.001$ ), 3309C ( $p <$

396 0.001) and SO4 ( $p < 0.001$ ) (Supplemental Figure 5B). Moreover, PC1 captured subtle variation in the  
397 leaf position by phenological stage interaction where middle leaves showed significant differences  
398 between anthesis and veraison ( $p < 1e-03$ ), and the oldest leaves showed significant differences when  
399 comparing anthesis to veraison ( $p < 1e-05$ ) and anthesis to harvest ( $p < 1e-03$ ).

400 For PC2, 61.4% of variation could be assigned to an experimental factor. This included  
401 significant variation from leaf position (46.9%,  $\text{padj} < 1e-05$ ), phenology (1.4%;  $\text{padj} < 1e-05$ ), and the  
402 interaction of leaf position and phenology (12.05%;  $\text{padj} < 1e-05$ ; Figure 4D). Specifically, younger  
403 leaves tended to have shallower sinuses and exaggerated superior sinus depths (higher values on PC2),  
404 whereas older leaves tended to develop deeper petiolar sinuses and more shallow superior sinuses (lower  
405 values on PC2). The degree of this separation decreased across the season, and the shapes converged on  
406 the mean leaf shape on PC2, consistent with the middle leaf at all three phenological stages. PC2  
407 additionally reflected the interaction of leaf position and rootstock (0.22%;  $p = 0.04$ ; Supplemental Figure  
408 5B), but post-hoc comparisons did not find any significant pairwise comparisons.

409 Machine learning on the GPA-rotated coordinate space identified moderate division of  
410 developmental and phenological classes. Random forest models could predict the leaf position with  
411 73.1% accuracy, with the most important feature being the y-component of the leaf apex ( $\text{MDA} = 0.051$ ).  
412 A model trained to predict phenology performed at 64.3% with the most important features being the x-  
413 components of the points corresponding to superior sinus depth (left sinus  $\text{MDA} = 0.030$ , right sinus  
414  $\text{MDA} = 0.019$ ). A model trained to predict rootstock performed only marginally better than chance at  
415 28.1% accuracy.

#### 416 417 *Vine physiology*

418 We measured intracellular  $\text{CO}_2$  concentration ( $C_i$ ), stomatal conductance ( $g_s$ ), leaf transpiration,  
419 water potential ( $\psi$ ), and soil moisture for the 72-vine set (Figure 5). Each physiological phenotype varied  
420 significantly across phenology and the block by phenology interaction (Figure 5A). For example, at  
421 harvest, we observed specific differences in leaf  $\text{CO}_2$  concentration (A vs C:  $p=0.003$ ; B vs C:  $p=0.002$ )

422 and leaf transpiration (A vs B:  $p < 1e-03$ ; A vs C:  $p < 1e-05$ ; B vs C:  $p < 1e-05$ ). Leaf transpiration and  
423 stomatal conductance varied significantly with the interaction of rootstock and phenology. A post-hoc  
424 comparison of means showed that leaf transpiration and stomatal conductances were elevated in  
425 'Chambourcin' vines grafted to '1103P' at veraison as compared to leaves of ungrafted vines (leaf  
426 transpiration:  $p = 0.001$ ; stomatal conductance:  $p = 0.002$  Figure 5B-C).

427

428

#### 429 *Phenomic covariation*

430 Four leaf phenotyping modalities consisted of 10 or more measured phenotypes and were  
431 measured for all plants in the 72-vine set (leaf ionome, leaf metabolomics, gene expression, leaf shape).  
432 Using these data, we explored the extent to which different phenotypes (within and between modalities)  
433 covaried over phenology and rootstock genotype (Figure 6; Supplemental Figure 6; Supplemental Figure  
434 7). Within each phenotyping modality, we summarized the primary dimensions of phenotypic variation  
435 using PCA (see Methods), so as to not weigh any modality too heavily. From each PCA, we extracted the  
436 top 10 PCs, which explained a total of 88.9% of variation in the ionomics PCA (iPCA), 55.9% of the  
437 variation for the metabolomics PCA (mPCA), 74.8% of the variation in the gene expression PCA (gPCA)  
438 and 87.9% of the variation in the leaf shape PCA (sPCA).

439 Pairwise correlations of each PC within each phenological stage showed diverse correlation  
440 magnitudes and directions both within a phenotyping modality and between phenotyping modalities  
441 (Figure 6A-C; Supplemental Figure 6). Generally, the strongest relationships were between PCs within  
442 phenotyping modalities. For example, the strongest correlations identified were between gene expression  
443 PCs gPC1 and gPC2 at anthesis ( $r = 0.85$ , CI = [0.81, 0.87]; Supplemental Figure 6A, and metabolomics  
444 PCs mPC1 and mPC2 at harvest ( $r = -0.78$ , CI = [-0.82, -0.76]). Correlations between modalities  
445 represented a diversity of responses across phenological stages. For example, the correlation between  
446 gene expression gPC4 and shape sPC3 was similar across the phenological stages, but only the correlation  
447 at veraison was significant ( $r = 0.41$ , CI = [0.34, 0.47]; Supplemental Figure 6B). Correlations such as



448 between metabolomics mPC3 and gene expression gPC6 were similar and significant at both veraison ( $r =$   
449  $-0.44$ ,  $CI = [-0.50, -0.37]$ ; Supplemental Figure 6C) and harvest ( $r = -0.37$ ,  $CI = [-0.45, -0.28]$ ;  
450 Supplemental Figure 5C). While many correlations varied over the course of the season, some  
451 relationships entirely shifted in direction. For example, the correlation between metabolomics mPC3 and  
452 mPC6 shifted from a positive significant relationship ( $r = 0.58$ ,  $CI = [0.52, 0.63]$ ) at veraison to a negative  
453 significant relationship at veraison ( $r = -0.66$ ,  $CI = [-0.73, -0.59]$ ) (Supplemental Figure 6D).

454 Pairwise comparisons of PCs within each rootstock genotype show a suite of latent phenotypes  
455 with significant presence/absence variation in significant correlations. Where each phenological stage  
456 showed modularity by phenotyping modality, variation over rootstock genotype shows a strong ionomics  
457 module with latent combination of other modalities interspersed (Supplemental Figure 7). For example, in  
458 ungrafted vines, metabolomics mPC1 was correlated with four PCs from the ionome (Supplemental  
459 Figure 7A). Each of the other rootstock genotypes had dramatically different topologies with the ionome  
460 tending to be more connected within the ionome and connected to other modalities only on the periphery  
461 (Supplemental Figure 7B-D). Examples of presence/absence variation were shown in small modules of  
462 two latent phenotypes that were present in only one rootstock genotype. For example, in the ungrafted  
463 vines, the correlation between gene expression gPC4 and metabolomics mPC3 was significant ( $r = -0.58$ ,  
464  $CI = [-0.65, -0.51]$ ) and, in '1103P'-grafted vines, the correlation between metabolomics mPC3 and shape  
465 sPC6 ( $r = 0.59$ ,  $CI = [0.53, 0.70]$ ) was significant.

466

## 467 Discussion

468

469 In this study, we used grafted grapevines as an experimental system for characterizing root system  
470 impacts on multi-dimensional leaf phenotypes over the course of a growing season. We detected  
471 ubiquitous but subtle effects of the root system on all assayed modalities, and demonstrated that rootstock  
472 influences on leaf phenotypes can be specific to the vine's developmental stage. The strongest signals of

473 rootstock influences on leaves were observed in the ionomics dataset, phenotypes for which the root  
474 system has a noted and well-understood role.

475

476 *Phenology explains significant variation in all leaf phenotypes*

477 The timing of sampling or phenological stage of the vines (anthesis, veraison, harvest) was the  
478 strongest driver of phenomic variation for most leaf phenotypes. For example, all 20 ions varied with  
479 phenology and most ions showed that phenology, or the interaction of phenology with leaf developmental  
480 position, was the strongest source of variation (Figure 1). Nearly one third of all measured transcripts  
481 responded to seasonal variation, and the strongest effects on the transcriptome were phenology and row, a  
482 correlate for the time within a three-hour sampling window. The only phenotype for which phenology  
483 was not the most explanatory factor is leaf shape. Consistent with previous studies [23][23], we confirm  
484 that most of the leaf shape variation reflects development along a single shoot, but much of this variation  
485 is explained via interaction with phenology. These data highlight the dynamic nature of biological  
486 processes taking place within grapevines over the course of a season.

487 The seasonal component to grapevine phenomic variation is a subject of much research,  
488 especially in the berry. In studies designed to quantify molecular underpinnings of terroir, seasonal  
489 variation was identified as the strongest signal in the metabolome [51–54],[51–54]. Several studies have  
490 characterized transcriptomic variation over the course of the season. For example, in conjunction with  
491 metabolomics, seasonal variation of berry development was used to identify transcriptomic and  
492 metabolomic developmental markers in ‘Corvina’ [55],[55]. Follow-up analysis showed that nearly 18%  
493 of transcripts varied seasonally [56],[56]. Grapevine leaf shape also varies tremendously over the growing  
494 season [23][23] and is stable over multiple growing seasons; interestingly, grapevine leaves are patterned  
495 in the previous year, and the climate of the season in which the leaves were patterned influence aspects of  
496 leaf shape [57,58],[57,58].

497

498 *Grafting and rootstock genotype exhibit a complex and subtle signal on leaf phenotypes*

499 Consistent with previous studies, we confirm that grafting, as well as rootstock genotype, has a  
500 complex effect on phenomic variation in the scion (the grafted shoot system). Most notably, we show that  
501 the rootstock to which a scion is grafted influences ion concentrations in leaves. Rootstock genotype is  
502 predictable from ion concentrations in the leaves, and this signal is strengthened when phenological stage  
503 is included in the model. For example, we previously showed that nickel concentration was elevated in  
504 vines grafted to the rootstock 'SO4' ~~[49]~~[19]. At a similar point in the season, we observe the same  
505 pattern, but by harvest, nickel was almost entirely excluded from the leaf. This suggests that the  
506 biological implications of this differential uptake could be missed if not surveyed across the season. We  
507 also confirm that rootstock genotype influences the metabolome of grafted grapevine, in some cases in a  
508 season-specific manner. In the transcriptome, PCA was able to identify dimensions of variation that were  
509 significantly described by rootstock and the interaction of rootstock and time of day, confirming prior  
510 observations ~~[49]~~[19]. Patterns of gene expression were associated with rootstock in some analyses; for  
511 example, supervised methodologies identified linear discriminants in the PC space that separated gene  
512 expression ~~patterns~~ of some rootstock genotypes. However, gene-by-gene analysis found no genes  
513 modulated by rootstock genotype, or even just from the act of grafting that were not driven entirely by a  
514 single outlier. We suspect these results are due, at least in part, to the strength of the phenology effect  
515 overpowering more subtle variation imparted by rootstock genotype. Finally, of the physiology  
516 phenotypes we measured, leaf transpiration and stomatal conductance were higher in vines grafted to  
517 '1103P' in the middle of the season. Through these analyses, we have identified subtle but ubiquitous  
518 effects of rootstock genotype on shoot system phenotype across modalities, and have shown that the  
519 impact of grafting on leaf phenomic variation varies from one phenotype to the next.

520 Understanding the rootstock genotype influence on shoot system phenotypes is a growing area of  
521 research, especially in grapevine. For example, in 'Cabernet Sauvignon', grafting increased ion uptake  
522 globally and some rootstock genotypes provide a clear signal in the scion ~~[28,59]~~[28]. The wild *Vitis*  
523 species from which the rootstocks were derived from (*Vitis berlandieri*, *V. riparia*, and *V. rupestris*) differ

524 in root architecture, preferred soil substrate, and genetic background; however, the specific aspects of  
525 their biology that contribute to differences in ion uptake are not known [27]. To our knowledge, there is  
526 not yet a strong causal link between the micronutrient component of the ionome and factors of vine  
527 growth or development that might influence traits like wine quality. However, it is noted that  
528 macronutrient deficiencies can have negative effects on such traits ~~{60,61}~~[59,60] and can be mediated by  
529 rootstock ~~{62}~~[61]. This suggests a strong understanding of the rootstock influence on the vine's ionome  
530 is warranted, and more work needs to be done to establish these relationships. Similarly, the metabolome  
531 is a key driver of the formation of the graft junction and some key metabolites could be responsible for  
532 graft incompatibility ~~{63}~~[62]. Building on this work, targeted metabolomics showed two classes of  
533 metabolites, flavanols and stilbenes, were differentially abundant at graft junctions and in the rootstocks  
534 of 'Cabernet Sauvignon' vines one month after grafting ~~{64}~~[63]. However, flavanols were not  
535 differentially abundant in the scion, but scion stilbene concentrations were apparently controlled by  
536 rootstock genotype. The effect of rootstock genotype on the scion transcriptome is perhaps the most  
537 varied. For example, 'Cabernet Sauvignon' shoot apical meristems show no effects by rootstock genotype  
538 ~~{44}~~[14], but berries of the same cultivar do, although the effect is tempered by seasonal variation  
539 ~~{5}~~[15]. Variation in 'Chambourcin' leaf shape was also driven by rootstock genotype, especially in  
540 conjunction with differences in irrigation ~~{19}~~[19]. Collectively, these studies all suggest that rootstock  
541 genotype influences scion phenotypes, but those effects will vary by phenotype, scion genotype, and  
542 perhaps other experimental conditions.

543 Data presented here confirm and expand upon previous observations of rootstock effects on scion  
544 phenotypes. Notably, this study was carried out using a robust experimental design (288-vine set and 72-  
545 vine set comprising replicates of three rootstocks grafted with a common scion and an ungrafted control)-  
546 in a vineyard that had been in the ground for eight years at the time of sampling. Our coordinated  
547 collection of five multi-dimensional leaf phenotypes, and inclusion of three sampling points spanning the  
548 growing season allowed us to investigate ~~in~~ the comprehensive nature of rootstock influences on the  
549 scion. Further, this thorough analysis demonstrates that rootstock effects on scion phenotypes shift in

550 magnitude over the course of the season, indicating that aspects of time are tremendously influential to  
551 the observed results regardless of phenotype.

552 While the results of previous studies on grafted grapevine are worthy of comparison, the work  
553 presented here has a few limitations that render comparisons with other studies challenging for a variety  
554 of reasons. One novelty in our study is the exploration of a hybrid grapevine system, ‘Chambourcin’.  
555 ‘Chambourcin’ has a complex pedigree, including contributions from *Vitis riparia* and *V. rupestris*,  
556 species which are each parent to two of the rootstocks used in this study [65]-[64]. Many of the significant  
557 effects we observed in this study were subtle, which could reflect the genomic similarity between shoot  
558 and root systems. It might be expected that rootstocks derived from *V. riparia*, *V. rupestris* and other  
559 North American species might prompt more pronounced responses in European scions that lack North  
560 American *Vitis* in their pedigrees. Moreover, our results were derived from data collected in a single year  
561 at a single location. The phenotypes we measured are known to be heavily influenced by the environment,  
562 and we expect some inter-annual variation in rootstock influences on shoot system phenotypes. This study  
563 focused on a single scion, and as a result we are unable to explore how rootstock effects on shoot system  
564 phenotypes vary across scions. To our knowledge, this is among the largest populations to have been  
565 surveyed for such phenotypes in a near-decade-old established vineyard. While many studies have been  
566 conducted in green houses or recently planted vineyards, the juxtaposition of our results and those  
567 previously established serve as a powerful foundation for the generation of hypotheses for future studies.

568  
569 *Phenomic covariation warrants work toward latent phenotypes*

570 In the present study, we assess the extent of covariation among leaf phenotypes. For the primary  
571 dimensions of variation in each modality, within-modality correlations ~~are~~were strongest when  
572 accounting for phenological timing. Correlations also ~~exist~~existed between modalities, suggesting room  
573 for the analysis of latent phenomic structure or targeted integrative analyses for experimental questions.  
574 For example, aspects of the metabolome were frequently correlated with the transcriptome and leaf shape  
575 when accounting for both phenological stage and rootstock genotype. Interestingly, correlations within

576 and between modalities were highly dynamic over a growing season and across rootstock genotype. For  
577 example, several correlations with leaf shape were present at veraison, but were not detected at anthesis  
578 and harvest. Moreover, the topology of connections in the ionic network was variable over the  
579 rootstock genotype (Supplemental Figure 6). This variation in topology confirms that root system  
580 genotype has a strong influence on shoot system elemental composition, and suggests that root system  
581 genotype can alter correlative patterns in the ionome. We believe phenomic covariation warrants further  
582 investigation, specifically, by further including additional phenotypes such as lncRNA expression ~~[66,67],~~  
583 ~~epigenetics [68], and microbiomes [69,70][65,66], epigenetics [67], and microbiomes [68,69]~~ which  
584 could yield more mechanistic understandings of the influence of root systems on shoot systems and how  
585 plants interact with their environments through their root systems. These mechanistic understandings  
586 could be used to further understand and optimize consumer-facing traits such as fruit quality and yield. To  
587 date, much of the work constituting phenomics in grapevine has addressed how berries develop over the  
588 growing season, how cultivars differ from one another, and how the concept of terroir influences wine  
589 ~~[51,52,55,71-73],[51,52,55,70-72]~~. Despite data integration techniques becoming more popular, there are  
590 still many open questions as to what analytical methods are most appropriate and how to most effectively  
591 utilize them (reviewed for grapevine in ~~[74,75][73,74]~~; reviewed broadly in ~~[76,77][75,76]~~). Ongoing  
592 work attempts to integrate high-dimensional phenomic datasets generated within a single organ system  
593 (e.g., leaves); and future studies will expand this to explore phenomic covariation in and among organs,  
594 over time, and across space.

595

### 596 **Potential Implications**

597 Our work on the influence of root system genotype on shoot system phenotype has broad  
598 implications for a holistic understanding of how plants detect and respond to changing environmental  
599 conditions, and how this response is coordinated among different organ systems. Data presented here  
600 demonstrate that root systems that are genetically distinct from the scion exert influence on the scion,  
601 leading to statistically significant differences in scion phenotypes based on the identity of their root



602 systems. This observation suggests that the above-ground phenotype ~~of plants~~ results, at least in part,  
603 from below-ground activity of the root system. Further, these data highlight the value of coordinated  
604 collection of different multi-dimensional phenotypes for comparative studies, and for describing whole-  
605 plant phenotypic shifts over seasons and in response to horticultural manipulations.

606 Beyond its use as an experimental model that is ideal for studying root/shoot interaction, grafting  
607 is an important horticultural technique that is used in over 70 major crops. In grapevines, grafting was  
608 developed primarily to combat the below-ground pest phylloxera, and grapevine rootstocks were selected  
609 initially based on their resistance to this pest. Results presented here indicate that beyond phylloxera  
610 resistance, grafting to genetically distinct rootstocks is a potential source of variation for the scion.  
611 Ongoing work explores how root system impacts on shoot system phenotypes vary across scion  
612 genotypes, and how the rootstock  $\times$  scion interaction changes over space. The long-term implications of  
613 this study are the potential honing of viticulture for future climates including the optimization of  
614 rootstock-scion combinations based in part on an understanding of how rootstock effects on scion  
615 phenotypes change over the course of the season. This work is relevant for breeding efforts, and may play  
616 a role in the optimization of quantitative phenotypes such as vigor, fruit quality, and yield that may be  
617 enhanced by, constrained by, or partially predicted from phenotypic variation elsewhere in the plant.

## 619 **Methods**

### 621 *Study Design*

622 Data were collected in 2017 from a split-plot experimental rootstock trial established in 2009 at  
623 the University of Missouri's Southwest Research Center near Mount Vernon, MO (37.074167 N;  
624 93.879167 W; Supplemental Figure 1). The rootstock trial includes the interspecific hybrid cultivar  
625 'Chambourcin' growing ungrafted (own-rooted) and grafted to three rootstocks: '1103P', '3309C', and  
626 'SO4' (Supplemental Figure 1D). Clonal replicates of each of the four rootstock-scion combinations were  
627 planted 72 times for a total of 288 vines planted in nine rows. Each row was treated with one of three

628 irrigation treatments: full evapotranspiration replacement, partial (50%) evapotranspiration replacement  
629 (reduced deficit irrigation; RDI), or no evapotranspiration replacement (Supplemental Figure 1A).  
630 However, rainfall in 2017 likely mitigated the applied irrigation treatment (see Supplemental Note 1).  
631 Vine position in the vineyard corresponded to time of sampling for some phenotypes (metabolomics, gene  
632 expression, and physiology), as samples were taken from one end of the vineyard to the other over the  
633 course of two to three hours. Because vineyard microclimates and sampling time may be associated with  
634 phenomic variation, we defined 'block' as a factor that captures this spatial and temporal variation  
635 inherent in sampling for those phenotypes. In the other phenotypes (ionomics and leaf shape), neither row  
636 nor block correlated with time, so 'block' was simply a spatial covariate. Unique rootstock-scion  
637 combinations were planted in cells of four adjacent replicated vines (Supplemental Figure 1A-B), with  
638 rows consisting of eight cells (32 vines/row). To our knowledge, a field-planted rootstock experimental  
639 vineyard of this size and age is rare. For some phenotypes (ionomics and leaf shape), it was possible to  
640 collect samples from all vines in the experimental vineyard (the 288-vine set; Supplemental Figure 1A-  
641 B). For other phenotypes (metabolomics, gene expression, and physiology), time and/or expense  
642 associated with the phenotyping process required that we reduce sampling to a nested set of 72 vines  
643 representing the middle two vines in each four-vine cell in the front half of the vineyard (the 72-vine set;  
644 Supplemental Figure 1B-C). All phenotypes were assayed at three phenological stages: anthesis (~80% of  
645 open flowers; 22 May 2017); veraison (~50% of berries had transitioned from green to red; 30 July 2017);  
646 and immediately prior to harvest (25 September 2017). At each phenological stage, effort was made to  
647 sample on days with full to partial sun and minimal precipitation.

648 This design was used to assess the following questions: 1) What is the influence of root system  
649 genotype on shoot system phenotype? 2) How do systems of plant phenotypes vary over the growing  
650 season and does rootstock genotype influence this variation? And 3) how do phenotypes covary within  
651 and between phenotyping modalities?

652

### 653 *Linear Models*

654 Linear models were fit to the 20 measured ion concentrations, the top 20 PCs of the leaf  
655 metabolome, the top 100 PCs of the leaf transcriptome, the top 20 PCs of leaf morphospace, and each  
656 measured physiological trait. Outliers were detected using the R function ‘anomalize’ (options:  
657 alpha=0.03, max\_anoms=0.1). Each model was fit with fixed effect factors representing phenological  
658 stage (anthesis, veraison, or harvest), rootstock (Ungrafted, ‘1103P’, ‘3309C’, or ‘SO4’), leaf position  
659 (youngest, middle, or oldest; only used in leaf morphology and leaf ion concentration models), and all  
660 pairwise interactions of those terms. Both irrigation and block were included as fixed, non-interacting  
661 effects with the exceptions of physiology and metabolomics, for which we allowed the interaction of  
662 ‘Block’ as it correlates with the time of sampling, potentially capturing temporal variation. Row, an  
663 additional correlate for time and spatial variation, was included in place of a temporal block for the gene  
664 expression models after removal of the variation attributable to irrigation, a factor collinear with row. All  
665 linear models were interpreted using a type-3 sum of squares computation using the R package ‘car’  
666 ~~{78}~~[\[77\]](#). Estimated p-values for each term in the models were corrected for multiple tests (within  
667 phenotype) using FDR correction as implemented by the R package ‘stats’ ~~{79}~~[\[78\]](#). Results from the  
668 models are reported as the variation explained by a particular term in the model and the estimated p-value.  
669 When appropriate, post-hoc mean comparisons were computed using the package ‘emmeans’ ~~{80}~~[\[79\]](#).  
670 Where multiple linear models were being simultaneously interpreted, we applied a Bonferonni correction  
671 to reduce the number of false positives.

672

### 673 *Machine Learning to Identify Rootstock Effects*

674 For visualization of between-class variation, we fit linear discriminant analysis models (LDA) to  
675 each modality (ionomics, metabolomics, gene expression, and leaf morphology) using the ‘lda’ function  
676 of the R package ‘MASS’ ~~{84}~~[\[80\]](#). Projections of all samples into the LD space were plotted using  
677 ggplot2 ~~{82}~~[\[81\]](#). In addition, we employed machine learning to capture subtle experimental effects. We  
678 partitioned data from each modality into 80% training partitions and 20% testing partitions. Models were

679 fit to predict the phenological stage from which a sample was taken, the rootstock to which the scion was  
680 grafted, and the joint prediction of phenology and rootstock. We also tested the predictability of leaf  
681 position for ionomics and leaf shape, and the interaction of rootstock and leaf position for ionomics. We  
682 used the ‘randomForest’ [83][82] implementation of the random forest algorithm. Models were fit and  
683 tuned using the R package ‘caret’ [84][83]. Each performance was assessed using accuracy, with  
684 performance on each class being assessed using the balanced accuracy, the midpoint of class-wise  
685 sensitivity and specificity. Where appropriate, models were compared to ‘chance’, or the occurrence  
686 frequency of each class. Confusion matrices were visualized from the out-of-bag predictions using  
687 `ggplot2::ggplot2`. Important features were identified from the randomForest object based on a phenotype-  
688 specific mean decrease in model accuracy (MDA).

689

#### 690 *Phenomic trait covariation*

691 We extracted ionomics, metabolomics, gene expression, and leaf shape data for the youngest  
692 available leaf from the 72--vine\_set. Each data modality was summarized along the primary dimensions  
693 of variation using PCA. For each class, we extracted the top 10 PCs and fit Pearson’s correlations across  
694 all pairs of PCs at each phenological stage. P-values from computed correlations were corrected using the  
695 FDR method from the package ‘stats’ [85][84]. Correlations and their strengths were visualized using the  
696 R package ‘igraph’ [86][85]. Example correlations were reported after running 10,000 bootstrapped  
697 subsamples of 90% of data for paired phenotypes. From the distribution of estimated correlation  
698 coefficients, confidence intervals were computed from the 0.025 and 0.975 quantiles. A subset of example  
699 correlations were plotted using the R package ‘ggplot2’ [82].

700

#### 701 **Acknowledgments:**

702 This work was funded by the National Science Foundation Plant Genome Research Project 1546869. We  
703 thank members of the Miller Lab at Saint Louis University and the Donald Danforth Plant Science  
704 Center, members of the Kovacs Lab at Missouri State University, members of the Kwasniewski Lab at the

705 University of Missouri, and members Londo Lab at the USDA-ARS Grape Research Unit for vineyard  
706 sampling and sample processing. We express special thanks to Matthew Rubin and Elizabeth Kellogg at  
707 the Donald Danforth Plant Science Center for valuable comments on the manuscript. Finally, we thank  
708 the reviewers of this manuscript whose comments have led to clearer and more complete manuscript.

709

710 **Figure Legends:**

711 Figure 1: The ionome shows strong signal from rootstock genotype, leaf position, and phenological stage

712 (A) Percent variation captured in linear models fit to each of 20 ions measured in the ionomics pipeline.

713 Presence of a cell indicates the model term (top) was significant (FDR;  $p_{\text{adj}} < 0.05$ ) for that ion (left).

714 (B) Example ions shown to vary significantly by the interaction of leaf position (Y=Youngest,

715 M=Middle, O=Oldest) and phenological stage in parts per million. Boxes are bound by 25th and 75th

716 percentile with whiskers extending 1.5 IQR from the box. Significant changes are indicated by letters

717 above boxes, and are only meant for comparison within each phenological stage. Group means are

718 displayed with black squares. (C) Example ions shown to vary significantly by the interaction of

719 rootstock genotype and phenological stage in parts per million. Significant changes are indicated by

720 letters above boxes, and are only meant for comparison within each phenological stage. Boxes are bound

721 by 25th and 75th percentile with whiskers extending 1.5 IQR from the box. Group means are displayed

722 with black squares. (D) Standardized heatmap for out-of-bag (OOB) predictions by a random forest

723 trained to predict rootstock genotype, (E) the interaction between rootstock genotype by phenology, and

724 (F) the interaction between rootstock genotype and leaf position.

725

726 Figure 2: The metabolome is influenced by rootstock genotype, phenological stage, and time of sampling.

727 (A) Percent variation captured in linear models fit to each of the top 20 principal components of the

728 metabolome (661 measured metabolites). Presence of a cell indicates the model term (top) was significant

729 for that PC (left, percent variation explained by the PC in parentheses). (B) The distribution of projections

730 onto PC17, the strongest captured rootstock effect in the metabolome. Boxes are bound by the 25th and

731 75th percentiles with whiskers extending 1.5 IQR from the box. **(C)** Projections of all samples into the  
732 first two dimensions of a linear discriminant space trained to maximize variation between rootstock  
733 genotypes.

734  
735 Figure 3: Gene expression primarily responds to time of season and circadian correlates  
736 **(A)** Heatmap showing 500 genes with the highest variance following the filtering of lowly expressed  
737 genes and gene-by-gene variance stabilizing transformations (VST) ordered by example model factors  
738 (below). **(B)** Percent variation captured in linear models fit to the top 100 Principal Components of the  
739 VST-transformed gene-expression space. Presence of a cell indicates the model term (top) was significant  
740 for that PC (left, percent variation explained by the PC in parentheses). **(C)** Projections of all samples into  
741 the first two principal component dimensions to show that the largest descriptors of variation are due to  
742 phenology. **(D)** Projections of all samples into the first two dimensions of the linear discriminant space  
743 trained to maximize variation between the rows of the vineyard, and **(E)** rootstock genotype.

744  
745 Figure 4: Leaf shape variation is primarily determined by shoot position but changes over the season  
746 **(A)** Representative shapes showing leaf variation (-3 sd, mean, +3 sd) captured in each of the top 4  
747 principal components of the Generalized Procrustes Analysis-rotated leaf shapes. **(B)** Projections of all  
748 leaves into the first two dimensions of principal component space colored by the strongest determinant of  
749 variation in the top two PCs. **(C)** Projections of all leaves into the first two dimensions of a linear  
750 discriminant space trained to maximize variation between phenological stages. **(D)** Variation in leaf shape  
751 captured on PC2 shown by leaf position and phenological stage. Large points represent the mean of the  
752 group when projected onto PC2. Bars surrounding the mean show one standard deviation. Variation in  
753 each group is shown as a composite leaf trace scaled to a standard size and centered over the mean.

754  
755 Figure 5: Vine physiology varies with rootstock and the rootstock by phenology interaction

756 (A) Percent variation explained by model terms (top) from linear models fit to each of four physiology  
757 traits (left). (B) Variation in leaf transpiration rate for each rootstock genotype over the course of the  
758 season. Boxes are bound by the 25th and 75th percentiles with whiskers extending 1.5 IQR from the box.  
759 Significant changes are indicated by letters above boxes, and are only meant for comparison within each  
760 phenological stage. Group means are displayed with black squares. (C) Variation in stomatal conductance  
761 for each rootstock genotype over the course of the season. Boxes are bound by the 25th and 75th  
762 percentiles with whiskers extending 1.5 IQR from the box. Group means are displayed with black  
763 squares. Significant changes are indicated by letters above boxes, and are only meant for comparison  
764 within each phenological stage.

765

766 Figure 6: Phenomic covariation varies over the course of the season

767 Correlation networks showing patterns of covariation within and between phenotyping modalities. Nodes  
768 of the network are connected if they are significantly correlated (Pearson, FDR;  $p_{\text{adj}} < 0.05$ ). Edge  
769 thickness is proportional to the strength of correlation (multiplied by 16 for visibility). Edge color reflects  
770 the direction of the correlation where blue edges indicate positive correlations and orange edges indicate  
771 negative correlations. Modalities are indicated by a leading character and node color: ionomics (iPCs;  
772 purple), metabolomics (mPCs; pink), gene expression (gPCs; yellow), leaf shape (sPCs; green). Network  
773 topologies are shown for (A) anthesis, (B) veraison, and (C) harvest.

774

#### 775 **Figure Supplement Legends:**

776 Supplemental Figure 1: Experimental Design

777 (A) Vineyard Map. The vineyard features a randomized block design where ‘Chambourcin’ is grown  
778 ungrafted and grafted to three rootstock genotypes: ‘1103P’, ‘3309C’, and ‘SO4’. Each row is treated  
779 with one of three irrigation treatments: full replacement of ET, reduced-deficit, no replacement of ET.  
780 Each cell of the vineyard contains four replicate grafts. (B) Phenotype sampling scheme across the four  
781 replicates in a cell. For example, the top panel (purple) shows all four vines in the first cell of Row 8 in

782 Block D. From each vine in that cell, ionomics and leaf shape were sampled. In contrast, the lower panel  
783 shows the first cell in Row 8 in Block A. Here, the first and fourth replicates were sampled for ionomics  
784 and leaf shape while the second and third replicates were sampled for all phenotypes. All vines (288)  
785 were sampled for ionomics and leaf shape. The middle two vines in the front half of the vineyard (72  
786 ) were additionally sampled for metabolomics, gene expression, and physiology. (C) Phenotype sample  
787 scheme within a vine (along a shoot). For each plant, young leaves were sampled for ionomics, leaf  
788 shape, and gene expression. Middle leaves were sampled for ionomics, leaf shape, metabolomics, and  
789 physiology. Older leaves were sampled for ionomics and leaf shape. Samples for ionomics and leaf shape  
790 were taken from the same shoot. All other phenotypes were sampled from independent shoots. (D)  
791 Rootstock relatedness. Each of the rootstocks in this trial shares a parent species with a different  
792 rootstock. '1103P' is a cross between *Vitis rupestris* and *V. berlandieri*. '3309C' is a cross between *V.*  
793 *rupestris* and *V. riparia*. 'SO4' is a cross between *V. riparia* and *V. berlandieri*. The parent that is shared  
794 between each pair of rootstocks is highlighted. This figure is partially reproduced from [\[49\]\[19\]](#) available  
795 under a Creative Common license (CC BY 4.0).

796  
797 Supplemental Figure 2: Quality and validity assessment of 3' RNAseq data. (A) A survey of recently  
798 annotated circadian clock orthologs from the grapevine genome annotation [44]. Orthologs surveyed  
799 included the morning-phased RVE1 and LHY, evening-phased LUX and ELF4, and the nigh-phased  
800 TOC1 (B) A survey of genes with housekeeping domains related to IPR000626 (ubiquitin) and  
801 IPR004000 (actin).

802  
803 Supplemental Figure 3: Patterns of ion covariation change over experimental treatments  
804 Correlation networks showing patterns of ion covariation across phenological stages and shoot position.  
805 Nodes of the network are connected if they are significantly correlated (Pearson, FDR;  $p_{adj} < 0.05$ ).  
806 Edge thickness is proportional to the strength of correlation (multiplied by 16 for visibility). Edge color



807 reflects the direction of the correlation where blue edges indicate positive correlations and orange edges  
808 indicate negative correlations.

809

810 Supplemental Figure 4: Patterns of variation contributing to gene expression linear discriminants

811 **(A)** Projections of leaf gene expression samples into the first two dimensions of a linear discriminant  
812 space trained to maximize variation between phenological stages, rows in the vineyard, and rootstock  
813 genotype. For each LD, the PCs that loaded significantly ( $>1.96$  sd from the mean loading) are listed in  
814 order of loading magnitude. **(B)** Distribution of the top loading PCs onto LD1 and LD2 for each of the  
815 trained models.

816

817 Supplemental Figure 5: Patterns of variation in leaf shape are subtle

818 **(A)** Percent variation captured in linear models fit to each of the top 20 principal components of leaf  
819 morphology. Presence of a cell indicates the model term (top) was significant for that PC (left, percent  
820 variation explained by the PC in parentheses). **(B)** Composite leaf traces for the main rootstock genotype  
821 effect identified on PC1.

822

823 Supplemental Figure 6: Example correlations within and between phenotyping modalities over the course  
824 of the season

825 **(A)** Example correlation showing a strong within-modality correlation between the ionomics gPC1 and  
826 gPC2 at anthesis. Pearson correlations by phenological stage and CIs derived from 10000 random 90%  
827 draws are shown for each panel. Generally speaking, CIs overlapping with 0 were not accepted as  
828 significant. **(B)** Example correlation showing one of the stronger between-modality correlations between  
829 the gene expression gPC4 and morphology (shape) sPC3 at veraison. **(C)** Example correlation of a  
830 relationship that is present multiple times over the course of the season between metabolomics mPC3 and

831 gene expression gPC6 at both veraison and harvest. **(D)** Example correlation that is dynamic over the  
832 course of the growing season between the ionomics mPC3 and mPC6.

833

834 Supplemental Figure 7: Phenomic covariation varies over rootstock genotype

835 Correlation networks showing patterns of covariation within and between phenotyping modalities. Nodes  
836 of the network are connected if they are significantly correlated (Pearson, FDR;  $p_{\text{adj}} < 0.05$ ). Edge  
837 thickness is proportional to the strength of correlation (multiplied by 16 for visibility). Edge color reflects  
838 the direction of the correlation where blue edges indicate positive correlations and orange edges indicate  
839 negative correlations. Modalities are indicated by a leading character and node color: ionomics (iPCs;  
840 purple), metabolomics (mPCs; pink), gene expression (gPCs; yellow), leaf shape (sPCs; green). Network  
841 topologies are shown for **(A)** Ungrafted, **(B)** '1103P'-grafted vines, **(C)** '3309C'-grafted vines, and **(D)**  
842 'SO4'-grafted vines.

843

#### 844 **Availability of Data:**

845 Ionomics data are available at <https://dx.doi.org/10.6084/m9.figshare.13200980>. Metabolomics data are  
846 available at <https://dx.doi.org/10.6084/m9.figshare.13201043>. Gene expression data are available in the  
847 Sequence Read Archive under BioProject PRJNA674915. Leaf scans and leaf landmarks are available at  
848 <https://dx.doi.org/10.6084/m9.figshare.13200953>. Weather and physiology data are available at  
849 <https://dx.doi.org/10.6084/m9.figshare.13198682> and <https://dx.doi.org/10.6084/m9.figshare.13201016>,  
850 respectively.

851

#### 852 **Availability of Code:**

853 All code for this paper including shell scripts for RNAseq analysis and Jupyter Notebooks for data  
854 analysis in R can be found on the Vitis Underground GitHub  
855 ([https://github.com/PGRP1546869/mt\\_vernon\\_2017\\_leaf](https://github.com/PGRP1546869/mt_vernon_2017_leaf)).

856

857 **Author Contributions:**

858 AJM, DHC, AF, LGK, MK, JPL, and QM designed the experiment. ZNH, LLK, MA, JFS, ZM, NB, EF,  
859 and JPL contributed to sample collection and sample processing. ZNH, LLK, JFS, and MA contributed to  
860 data analysis. ZNH and AJM contributed to the writing of the manuscript. All authors contributed to  
861 manuscript editing.

862

863 **References:**

- 864 1. Gehan MA, Fahlgren N, Abbasi A, Berry JC, Callen ST, Chavez L, et al.. PlantCV v2: Image analysis  
865 software for high throughput plant phenotyping. *PeerJ*. 5:e40882017;
- 866 2. Ubbens JR, Stavness I. Deep Plant Phenomics: A Deep Learning Platform for Complex Plant  
867 Phenotyping Tasks. *Front Plant Sci*. 8:11902017;
- 868 3. Ubbens J, Cieslak M, Prusinkiewicz P, Stavness I. Latent Space Phenotyping: Automatic Image Based  
869 Phenotyping for Treatment Studies.
- 870 4. Soulé M. PHENETICS OF NATURAL POPULATIONS I. PHENETIC RELATIONSHIPS OF  
871 INSULAR POPULATIONS OF THE SIDE BLOTCHED LIZARD. *Evolution*. 21:584-911967;
- 872 5. Houle D, Govindaraju DR, Omholt S. Phenomics: the next challenge. *Nat Rev Genet*. 11:855-662010;
- 873 6. Mudge K, Janick J, Seofield S, Goldschmidt EE. A History of Grafting. In: Janick J, editor.  
874 *Horticultural Reviews*. Hoboken, NJ, USA: John Wiley & Sons, Inc.; p. 437-93.
- 875 7. Pouget R. Histoire de la lutte contre le phylloxéra de la vigne en France: 1868-1895. *Hist Sci Med*.  
876 INRA; 1990;
- 877 8. Walker MA, Lund K, Agüero C, Riaz S, Fort K, Heinitz C, et al.. BREEDING GRAPE  
878 ROOTSTOCKS FOR RESISTANCE TO PHYLLOXERA AND NEMATODES—IT'S NOT ALWAYS  
879 EASY. *Acta Horticulturae*.
- 880 9. Warschefsky EJ, Klein LL, Frank MH, Chitwood DH, Londo JP, von Wettberg EJB, et al.. Rootstocks:  
881 Diversity, Domestication, and Impacts on Shoot Phenotypes. *Trends Plant Sci*. Elsevier Current Trends;  
882 21:418-372016;
- 883 10. Tramontini S, Vitali M, Centioni L, Schubert A, Lovisolo C. Rootstock control of scion response to  
884 water stress in grapevine. *Environmental and Experimental Botany*.
- 885 11. Bavareseo L, Lovisolo C. Effect of grafting on grapevine chlorosis and hydraulic conductivity. *VITIS*  
886 *Journal of Grapevine Research*. Citeseer; 2015;
- 887 12. Ferlito F, Distefano G, Gentile A, Allegra M, Lakso AN, Nicolosi E. Scion-rootstock interactions  
888 influence the growth and behaviour of the grapevine root system in a heavy clay soil. *Australian Journal*  
889 *of Grape and Wine Research*.

- 890 [13. Ordish G. The great wine blight. J.M. Dent & Sons;](#)
- 891 [14. Cookson SJ, Ollat N. Grafting with rootstocks induces extensive transcriptional re-programming in](#)  
892 [the shoot apical meristem of grapevine. \*BMC Plant Biol.\* BioMed Central; 13:1–142013;](#)
- 893 [15. Corso M, Vannozzi A, Ziliotto F, Zouine M, Maza E, Nicolato T, et al.. Grapevine Rootstocks](#)  
894 [Differentially Affect the Rate of Ripening and Modulate Auxin-Related Genes in Cabernet Sauvignon](#)  
895 [Berries. \*Front Plant Sci.\* Frontiers; 2016; doi: 1. Gehan MA, Fahlgren N, Abbasi A, Berry JC, Callen ST,](#)  
896 [Chavez L, et al.. PlantCV v2: Image analysis software for high-throughput plant phenotyping. \*PeerJ.\*](#)  
897 [5:e40882017;](#)
- 898 [2. Ubbens JR, Stavness I. Deep Plant Phenomics: A Deep Learning Platform for Complex Plant](#)  
899 [Phenotyping Tasks. \*Front Plant Sci.\* 8:11902017;](#)
- 900 [3. Ubbens J, Cieslak M, Prusinkiewicz P, Stavness I. Latent Space Phenotyping: Automatic Image-Based](#)  
901 [Phenotyping for Treatment Studies.](#)
- 902 [4. Soulé M. PHENETICS OF NATURAL POPULATIONS I. PHENETIC RELATIONSHIPS OF](#)  
903 [INSULAR POPULATIONS OF THE SIDE-BLOTCHED LIZARD. \*Evolution.\* 21:584–911967;](#)
- 904 [5. Houle D, Govindaraju DR, Omholt S. Phenomics: the next challenge. \*Nat Rev Genet.\* 11:855–662010;](#)
- 905 [6. Mudge K, Janick J, Scofield S, Goldschmidt EE. A History of Grafting. In: Janick J, editor.](#)  
906 [Horticultural Reviews. Hoboken, NJ, USA: John Wiley & Sons, Inc.; p. 437–93.](#)
- 907 [7. Pouget R. Histoire de la lutte contre le phylloxéra de la vigne en France: 1868-1895. \*Hist Sci Med.\*](#)  
908 [INRA; 1990;](#)
- 909 [8. Walker MA, Lund K, Agüero C, Riaz S, Fort K, Heinitz C, et al.. BREEDING GRAPE](#)  
910 [ROOTSTOCKS FOR RESISTANCE TO PHYLLXERA AND NEMATODES - IT'S NOT ALWAYS](#)  
911 [EASY. \*Acta Horticulturae.\*](#)
- 912 [9. Warschewsky EJ, Klein LL, Frank MH, Chitwood DH, Londo JP, von Wettberg EJB, et al.. Rootstocks:](#)  
913 [Diversity, Domestication, and Impacts on Shoot Phenotypes. \*Trends Plant Sci.\* Elsevier Current Trends;](#)  
914 [21:418–372016;](#)
- 915 [10. Tramontini S, Vitali M, Centioni L, Schubert A, Lovisolo C. Rootstock control of scion response to](#)  
916 [water stress in grapevine. \*Environmental and Experimental Botany.\*](#)
- 917 [11. Bavaresco L, Lovisolo C. Effect of grafting on grapevine chlorosis and hydraulic conductivity. \*VITIS-\*](#)  
918 [Journal of Grapevine Research. Citeseer; 2015;](#)
- 919 [12. Ferlito F, Distefano G, Gentile A, Allegra M, Lakso AN, Nicolosi E. Scion–rootstock interactions](#)  
920 [influence the growth and behaviour of the grapevine root system in a heavy clay soil. \*Australian Journal\*](#)  
921 [of Grape and Wine Research.](#)
- 922 [13. Ordish G. The great wine blight. J.M. Dent & Sons;](#)
- 923 [14. Cookson SJ, Ollat N. Grafting with rootstocks induces extensive transcriptional re-programming in](#)  
924 [the shoot apical meristem of grapevine. \*BMC Plant Biol.\* BioMed Central; 13:1–142013;](#)
- 925 [15. Corso M, Vannozzi A, Ziliotto F, Zouine M, Maza E, Nicolato T, et al.. Grapevine Rootstocks](#)  
926 [Differentially Affect the Rate of Ripening and Modulate Auxin-Related Genes in Cabernet Sauvignon](#)

- 927 Berries. *Front Plant Sci.* Frontiers; 2016; doi: 10.3389/fpls.2016.00069.
- 928 16. Berdeja M, Nicolas P, Kappel C, Dai ZW, Hilbert G, Peccoux A, et al.. Water limitation and rootstock  
929 genotype interact to alter grape berry metabolism through transcriptome reprogramming. *Hortic Res.*  
930 2:150122015;
- 931 17. Zombaro A, Crosatti C, Bagnaresi P, Bassolino L, Reshef N, Puccioni S, et al.. Transcriptomic and  
932 biochemical investigations support the role of rootstock-scion interaction in grapevine berry quality. *BMC*  
933 *Genomics.* 21:4682020;
- 934 18. Chitarra W, Perrone I, Avanzato CG, Minio A, Boccacci P, Santini D, et al.. Grapevine Grafting:  
935 Scion Transcript Profiling and Defense-Related Metabolites Induced by Rootstocks. *Front Plant Sci.*  
936 Frontiers; 2017; doi: 10.3389/fpls.2017.00654.
- 937 16. Berdeja M, Nicolas P, Kappel C, Dai ZW, Hilbert G, Peccoux A, et al.. Water  
938 limitation and rootstock genotype interact to alter grape berry metabolism through transcriptome  
reprogramming. *Hortic Res.* 2:150122015;
- 939 17. Zombaro A, Crosatti C, Bagnaresi P, Bassolino L, Reshef N, Puccioni S, et al.. Transcriptomic and  
940 biochemical investigations support the role of rootstock-scion interaction in grapevine berry quality. *BMC*  
941 *Genomics.* 21:4682020;
- 942 18. Chitarra W, Perrone I, Avanzato CG, Minio A, Boccacci P, Santini D, et al.. Grapevine Grafting:  
943 Scion Transcript Profiling and Defense-Related Metabolites Induced by Rootstocks. *Front Plant Sci.*  
944 Frontiers; 2017; doi: 10.3389/fpls.2017.00654.
- 945 19. Migieovsky Z, Harris ZN, Klein LL, Li M, McDermaid A, Chitwood DH, et al.. Rootstock effects on  
946 scion phenotypes in a “Chambourcin” experimental vineyard. *Horticulture Research.* Nature Publishing  
947 Group; 6:1-132019;
- 948 20. Galet P. A Practical Ampelography: Grapevine Identification. Comstock Pub. Associates;
- 949 21. Mullins MG, Bouquet A, Williams LE. Biology of the Grapevine. Cambridge University Press;
- 950 22. Chitwood DH, Ranjan A, Martinez CC, Headland LR, Thiem T, Kumar R, et al.. A modern  
951 ampelography: a genetic basis for leaf shape and venation patterning in grape. *Plant Physiol.* 164:259-  
952 722014;
- 953 23. Chitwood DH, Klein LL, O’Hanlon R, Chacko S, Greg M, Kitchen C, et al.. Latent developmental  
954 and evolutionary shapes embedded within the grapevine leaf. *New Phytologist.*
- 955 24. Klein LL, Caito M, Chapnick C, Kitchen C, O’Hanlon R, Chitwood DH, et al.. Digital Morphometrics  
956 of Two North American Grapevines (*Vitis*: Vitaceae) Quantifies Leaf Variation between Species, within  
957 Species, and among Individuals. *Front Plant Sci.* 8:3732017;
- 958 25. Grimes DW, Williams LE. Irrigation Effects on Plant Water Relations and Productivity of Thompson  
959 Seedless Grapevines. *Crop Sci.* 30:2551990;
- 960 26. Williams LE, Grimes DW. Modelling vine growth development of a data set for a water balance  
961 subroutine. *Proceedings of the Sixth Australian Wine Industry Technical Conference.* p.169-74.
- 962 27. Gautier A, Cookson SJ, Lagalle L, Ollat N, Marguerit E. Influence of the three main genetic  
963 backgrounds of grapevine rootstocks on petiolar nutrient concentrations of the scion, with a focus on  
964 phosphorus. *OENO One.* 54:1-132020;

- 965 28. Lecourt J, Lauvergeat V, Ollat N, Vivin P, Cookson SJ. Shoot and root ionome responses to nitrate  
966 supply in grafted grapevines are rootstock genotype dependent: Rootstock and nitrogen supply affect  
967 grapevine ionome. *Aust J Grape Wine Res.* 21:311–82015;
- 968 29. Salt DE, Baxter I, Lahner B. Ionomics and the study of the plant ionome. *Annu Rev Plant Biol.*  
969 59:709–332008;
- 970 30. Baxter I. Ionomics: The functional genomics of elements. *Brief Funct Genomics.* 9:149–562010;
- 971 31. Ziegler G, Terauchi A, Becker A, Armstrong P, Hudson K, Baxter I. Ionomics Screening of Field-  
972 Grown Soybean Identifies Mutants with Altered Seed Elemental Composition. *The Plant Genome.*
- 973 32. Oliver SG, Winson MK, Kell DB, Baganz F. Systematic functional analysis of the yeast genome.  
974 *Trends Biotechnol.* 16:373–81998;
- 975 33. Tweeddale H, Notley McRobb L, Ferenci T. Effect of slow growth on metabolism of *Escherichia coli*,  
976 as revealed by global metabolite pool (“metabolome”) analysis. *J Bacteriol.* 180:5109–161998;
- 977 34. Islam MN, Downey F, Ng CKY. Comparative analysis of bioactive phytochemicals from *Scutellaria*  
978 *baicalensis*, *Scutellaria lateriflora*, *Scutellaria racemosa*, *Scutellaria tomentosa* and *Scutellaria wrightii* by  
979 LC-DAD-MS. *Metabolomics.* Springer; 7:446–532011;
- 980 35. Tautenhahn R, Patti GJ, Rinehart D, Siuzdak G. XCMS Online: a web-based platform to process  
981 untargeted metabolomic data. *Anal Chem.* 84:5035–92012;
- 982 36. Tandonnet S, Torres TT. Traditional versus 3’ RNA-seq in a non-model species. *Genom Data.* 11:9–  
983 162017;
- 984 37. Bolger AM, Lohse M, Usadel B. Trimmomatic: a flexible trimmer for Illumina sequence data.  
985 *Bioinformatics.* 30:2114–202014;
- 986 38. Bushnell B. BBTools software package. URL <http://sourceforge.net/projects/bbmap>. 2017;
- 987 39. Jaillon O, Aury J-M, Noel B, Polieriti A, Clepet C, Casagrande A, et al.. The grapevine genome  
988 sequence suggests ancestral hexaploidization in major angiosperm phyla. *Nature.* 449:463–72007;
- 989 40. Canaguier A, Grimplet J, Di-Gaspero G, Scalabrin S, Duchêne E, Choise N, et al.. A new version of  
990 the grapevine reference genome assembly (12X.v2) and of its annotation (VCost.v3). *Genom Data.*  
991 14:56–622017;
- 992 41. Dobin A, Davis CA, Schlesinger F, Drenkow J, Zaleski C, Jha S, et al.. STAR: ultrafast universal  
993 RNA-seq aligner. *Bioinformatics.* 29:15–212013;
- 994 42. Anders S, Pyl PT, Huber W. HTSeq: Analysing high-throughput sequencing data with Python.
- 995 43. Love MI, Huber W, Anders S. Moderated estimation of fold change and dispersion for RNA-seq data  
996 with DESeq2. *Genome Biol.* 15:5502014;
- 997 44. Carbonell Bejerano P, Rodríguez V, Royo C, Hernáiz S, Moro-González LC, Torres-Viñals M, et al..  
998 Circadian oscillatory transcriptional programs in grapevine ripening fruits. *BMC Plant Biol.* 14:782014;
- 999 45. Anders S, Huber W. Differential expression analysis for sequence-count data. *Genome Biol.*  
1000 11:R1062010;

- 1001 [46. Dryden IL, Mardia KV. Statistical Shape Analysis: With Applications in R. John Wiley & Sons;](#)
- 1002 [47. Shackel K, Gross R. Using midday stem water potential to assess irrigation needs of landscape valley](#)
- 1003 [oaks. 2002;](#)
- 1004 [48. Levin AD. Re-evaluating pressure chamber methods of water status determination in field-grown](#)
- 1005 [grapevine \(\*Vitis\* spp.\). \*Agric Water Manag.\* Elsevier BV; 221:422–92019;](#)
- 1006 [49. Liang W, Zou X, Carballar Lejarazú R, Wu L, Sun W, Yuan X, et al.. Selection and evaluation of](#)
- 1007 [reference genes for qRT-PCR analysis in \*Euscaphis konishii\* Hayata based on transcriptome data. \*Plant\*](#)
- 1008 [Methods. Springer Science and Business Media LLC; 2018; doi:-19. Migicovsky Z, Harris ZN, Klein LL,](#)
- 1009 [Li M, McDermaid A, Chitwood DH, et al.. Rootstock effects on scion phenotypes in a “Chambourcin”](#)
- 1010 [experimental vineyard. \*Hortic Res.\* 6:642019;](#)
- 1011 [20. Galet P. A Practical Ampelography: Grapevine Identification. Comstock Pub. Associates;](#)
- 1012 [21. Mullins MG, Bouquet A, Williams LE. Biology of the Grapevine. Cambridge University Press;](#)
- 1013 [22. Chitwood DH, Ranjan A, Martinez CC, Headland LR, Thiem T, Kumar R, et al.. A modern](#)
- 1014 [ampelography: a genetic basis for leaf shape and venation patterning in grape. \*Plant Physiol.\* 164:259–](#)
- 1015 [722014;](#)
- 1016 [23. Chitwood DH, Klein LL, O’Hanlon R, Chacko S, Greg M, Kitchen C, et al.. Latent developmental](#)
- 1017 [and evolutionary shapes embedded within the grapevine leaf. \*New Phytologist.\*](#)
- 1018 [24. Klein LL, Caito M, Chapnick C, Kitchen C, O’Hanlon R, Chitwood DH, et al.. Digital Morphometrics](#)
- 1019 [of Two North American Grapevines \(\*Vitis\*: Vitaceae\) Quantifies Leaf Variation between Species, within](#)
- 1020 [Species, and among Individuals. \*Front Plant Sci.\* 8:3732017;](#)
- 1021 [25. Grimes DW, Williams LE. Irrigation Effects on Plant Water Relations and Productivity of Thompson](#)
- 1022 [Seedless Grapevines. \*Crop Sci.\* 30:2551990;](#)
- 1023 [26. Williams LE, Grimes DW. Modelling vine growth-development of a data set for a water balance](#)
- 1024 [subroutine. \*Proceedings of the Sixth Australian Wine Industry Technical Conference.\* p. 169–74.](#)
- 1025 [27. Gautier A, Cookson SJ, Lagalle L, Ollat N, Marguerit E. Influence of the three main genetic](#)
- 1026 [backgrounds of grapevine rootstocks on petiolar nutrient concentrations of the scion, with a focus on](#)
- 1027 [phosphorus. \*OENO One.\* 54:1–132020;](#)
- 1028 [28. Lecourt J, Lauvergeat V, Ollat N, Vivin P, Cookson SJ. Shoot and root ionome responses to nitrate](#)
- 1029 [supply in grafted grapevines are rootstock genotype dependent: Rootstock and nitrogen supply affect](#)
- 1030 [grapevine ionome. \*Aust J Grape Wine Res.\* 21:311–82015;](#)
- 1031 [29. Salt DE, Baxter I, Lahner B. Ionomics and the study of the plant ionome. \*Annu Rev Plant Biol.\*](#)
- 1032 [59:709–332008;](#)
- 1033 [30. Baxter I. Ionomics: The functional genomics of elements. \*Brief Funct Genomics.\* 9:149–562010;](#)
- 1034 [31. Ziegler G, Terauchi A, Becker A, Armstrong P, Hudson K, Baxter I. Ionomics Screening of Field-](#)
- 1035 [Grown Soybean Identifies Mutants with Altered Seed Elemental Composition. \*The Plant Genome.\*](#)
- 1036 [32. Oliver SG, Winson MK, Kell DB, Baganz F. Systematic functional analysis of the yeast genome.](#)
- 1037 [Trends Biotechnol. 16:373–81998;](#)

- 1038 [33. Tweeddale H, Notley-McRobb L, Ferenci T. Effect of slow growth on metabolism of Escherichia coli,](#)  
1039 [as revealed by global metabolite pool \(“metabolome”\) analysis. \*J Bacteriol.\* 180:5109–161998;](#)
- 1040 [34. Islam MN, Downey F, Ng CKY. Comparative analysis of bioactive phytochemicals from \*Scutellaria\*](#)  
1041 [baicalensis, \*Scutellaria lateriflora\*, \*Scutellaria racemosa\*, \*Scutellaria tomentosa\* and \*Scutellaria wrightii\* by](#)  
1042 [LC-DAD-MS. \*Metabolomics.\* Springer; 7:446–532011;](#)
- 1043 [35. Tautenhahn R, Patti GJ, Rinehart D, Siuzdak G. XCMS Online: a web-based platform to process](#)  
1044 [untargeted metabolomic data. \*Anal Chem.\* 84:5035–92012;](#)
- 1045 [36. Tandonnet S, Torres TT. Traditional versus 3’ RNA-seq in a non-model species. \*Genom Data.\* 11:9–](#)  
1046 [162017;](#)
- 1047 [37. Bolger AM, Lohse M, Usadel B. Trimmomatic: a flexible trimmer for Illumina sequence data.](#)  
1048 [\*Bioinformatics.\* 30:2114–202014;](#)
- 1049 [38. Bushnell B. BBTools software package. URL <http://sourceforge.net/projects/bbmap>. 2017;](#)
- 1050 [39. Jaillon O, Aury J-M, Noel B, Policriti A, Clepet C, Casagrande A, et al.. The grapevine genome](#)  
1051 [sequence suggests ancestral hexaploidization in major angiosperm phyla. \*Nature.\* 449:463–72007;](#)
- 1052 [40. Canaguier A, Grimplet J, Di Gaspero G, Scalabrin S, Duchêne E, Choise N, et al.. A new version of](#)  
1053 [the grapevine reference genome assembly \(12X.v2\) and of its annotation \(VCost.v3\). \*Genom Data.\*](#)  
1054 [14:56–622017;](#)
- 1055 [41. Dobin A, Davis CA, Schlesinger F, Drenkow J, Zaleski C, Jha S, et al.. STAR: ultrafast universal](#)  
1056 [RNA-seq aligner. \*Bioinformatics.\* 29:15–212013;](#)
- 1057 [42. Anders S, Pyl PT, Huber W. HTSeq: Analysing high-throughput sequencing data with Python.](#)
- 1058 [43. Love MI, Huber W, Anders S. Moderated estimation of fold change and dispersion for RNA-seq data](#)  
1059 [with DESeq2. \*Genome Biol.\* 15:5502014;](#)
- 1060 [44. Carbonell-Bejerano P, Rodríguez V, Royo C, Hernáiz S, Moro-González LC, Torres-Viñals M, et al..](#)  
1061 [Circadian oscillatory transcriptional programs in grapevine ripening fruits. \*BMC Plant Biol.\* 14:782014;](#)
- 1062 [45. Anders S, Huber W. Differential expression analysis for sequence count data. \*Genome Biol.\*](#)  
1063 [11:R1062010;](#)
- 1064 [46. Dryden IL, Mardia KV. Statistical Shape Analysis: With Applications in R. John Wiley & Sons;](#)
- 1065 [47. Shackel K, Gross R. Using midday stem water potential to assess irrigation needs of landscape valley](#)  
1066 [oaks. 2002;](#)
- 1067 [48. Levin AD. Re-evaluating pressure chamber methods of water status determination in field-grown](#)  
1068 [grapevine \(\*Vitis\* spp.\). \*Agric Water Manag.\* Elsevier BV; 221:422–92019;](#)
- 1069 [49. Liang W, Zou X, Carballar-Lejarazú R, Wu L, Sun W, Yuan X, et al.. Selection and evaluation of](#)  
1070 [reference genes for qRT-PCR analysis in \*Euscaphis konishii\* Hayata based on transcriptome data. \*Plant\*](#)  
1071 [Methods. Springer Science and Business Media LLC; 2018; doi: 10.1186/s13007-018-0311-x.](#)
- 1072 [50. Podani J, Miklós I. Resemblance coefficients and the horseshoe effect in principal coordinates](#)  
1073 [analysis. \*Ecology.\* Wiley; 83:3331–432002;](#)



- 1074 51. Degu A, Hochberg U, Sikron N, Venturini L, Buson G, Ghan R, et al.. Metabolite and transcript  
1075 profiling of berry skin during fruit development elucidates differential regulation between Cabernet  
1076 Sauvignon and Shiraz cultivars at branching points in the polyphenol pathway. *BMC Plant Biol.*  
1077 14:1882014;
- 1078 52. Anesi A, Stocchero M, Dal Santo S, Commisso M, Zenoni S, Ceoldo S, et al.. Towards a scientific  
1079 interpretation of the terroir concept: plasticity of the grape berry metabolome. *BMC Plant Biol.*  
1080 15:1912015;
- 1081 53. Cuadros-Inostroza A, Ruiz-Lara S, González E, Eckardt A, Willmitzer L, Peña-Cortés H. GC-MS  
1082 metabolic profiling of Cabernet Sauvignon and Merlot cultivars during grapevine berry development and  
1083 network analysis reveals a stage- and cultivar-dependent connectivity of primary metabolites.  
1084 *Metabolomics.* 12:392016;
- 1085 54. Dal Santo S, Fasoli M, Negri S, D'Inca E, Vicenzi N, Guzzo F, et al.. Plasticity of the Berry Ripening  
1086 Program in a White Grape Variety. *Front Plant Sci.* 7:9702016;
- 1087 55. Zamboni A, Di Carli M, Guzzo F, Stocchero M, Zenoni S, Ferrarini A, et al.. Identification of putative  
1088 stage-specific grapevine berry biomarkers and omics data integration into networks. *Plant Physiol.*  
1089 154:1439–592010;
- 1090 56. Dal Santo S, Tornielli GB, Zenoni S, Fasoli M, Farina L, Anesi A, et al.. The plasticity of the  
1091 grapevine berry transcriptome. *Genome Biol.* 14:r542013;
- 1092 57. Chitwood DH, Rundell SM, Li DY, Woodford QL, Yu TT, Lopez JR, et al.. Climate and  
1093 Developmental Plasticity: Interannual Variability in Grapevine Leaf Morphology. *Plant Physiol.*  
1094 170:1480–912016;
- 1095 58. Chitwood DH, Mullins J, Migicovsky Z, Frank M, VanBuren R, Londo JP. Vein to blade ratio is an  
1096 allometric indicator of climate-induced changes in grapevine leaf size and shape. bioRxiv.
- 1097 59. Gautier A, Cookson SJ, Lagalle L, Ollat N, Marguerit E. Influence of the three main genetic  
1098 backgrounds of grapevine rootstocks on petiolar nutrient concentrations of the scion, with a focus on  
1099 phosphorus. *OENO One.* 54:1–132020;
- 1100 60. Bravdo B. EFFECT OF MINERAL NUTRITION AND SALINITY ON GRAPE PRODUCTION  
1101 AND WINE QUALITY. *Acta Horticulturae.* 512:23–302000;
- 1102 61. Brunetto G, Melo GWBDE, Toselli M, Quartieri M, Tagliavini M. The role of mineral nutrition on  
1103 yields and fruit quality in grapevine, pear and apple. *Rev Bras Frutic. FapUNIFESP (SciELO);* 37:1089–  
1104 1042015;
- 1105 62. Gautier A, Cookson SJ, Hevin C, Vivin P, Lauvergeat V, Mollier A. Phosphorus acquisition  
1106 efficiency and phosphorus remobilization mediate genotype-specific differences in shoot phosphorus  
1107 content in grapevine. *Tree Physiol.* Oxford University Press (OUP); 38:1742–512018;
- 1108 63. Canas S, Assunção M, Brazão J, Zanol G, Eiras-Dias JE. Phenolic compounds involved in grafting  
1109 incompatibility of *Vitis* spp: development and validation of an analytical method for their quantification.  
1110 *Phytochem Anal.* 26:1–72015;
- 1111 64. Prodhomme D, Valls Fonayet J, Hévin C, Franc C, Hilbert G, de Revel G, et al.. Metabolite profiling  
1112 during graft union formation reveals the reprogramming of primary metabolism and the induction of

- 1113 stilbene synthesis at the graft interface in grapevine. *BMC Plant Biol.* 19:5992019;
- 1114 65. Migieovsky Z, Sawler J, Money D, Eibach R, Miller AJ, Luby JJ, et al.. Genomic ancestry estimation  
1115 quantifies use of wild species in grape breeding. *BMC Genomics.* 17:4782016;
- 1116 66. Vitulo N, Foreato C, Carpinelli EC, Telatin A, Campagna D, D'Angelo M, et al.. A deep survey of  
1117 alternative splicing in grape reveals changes in the splicing machinery related to tissue, stress condition  
1118 and genotype. *BMC Plant Biol.* 14:992014;
- 1119 67. Harris ZN, Kovaes LG, Londo JP. RNA-seq based genome annotation and identification of long-  
1120 noncoding RNAs in the grapevine cultivar "Riesling." *BMC Genomics.* BioMed Central; 18:9372017;
- 1121 68. Williams BR, Edwards CE, Kwasniewski MT, Miller AJ. Epigenomic patterns reflect irrigation and  
1122 grafting in the grapevine clone 'Chambourcin'. *bioRxiv.* Cold Spring Harbor Laboratory; 2020;
- 1123 69. Maraseo R, Rolli E, Fusi M, Michoud G, Daffonchio D. Grapevine rootstocks shape underground  
1124 bacterial microbiome and networking but not potential functionality. *Microbiome.* 6:32018;
- 1125 70. Swift JP, Hall ME, Harris ZN, Kwasniewski MT, Miller AJ. Grapevine microbiota reflect diversity  
1126 among compartments and complex interactions within and among root and shoot systems. *bioRxiv.*
- 1127 71. Palumbo MC, Zenoni S, Fasoli M, Massonnet M, Farina L, Castiglione F, et al.. Integrated network  
1128 analysis identifies fight club nodes as a class of hubs encompassing key putative switch genes that induce  
1129 major transcriptome reprogramming during grapevine development. *Plant Cell. Am Soc Plant Biol;*  
1130 26:4617-352014;
- 1131 72. Savoi S, Wong DCJ, Arapitsas P, Miculan M, Bucchetti B, Peterlunger E, et al.. Transcriptome and  
1132 metabolite profiling reveals that prolonged drought modulates the phenylpropanoid and terpenoid  
1133 pathway in white grapes (*Vitis vinifera* L.). *BMC Plant Biol.* 16:672016;
- 1134 73. Savoi S, Wong DCJ, Degu A, Herrera JC, Bucchetti B, Peterlunger E, et al.. Multi-Omics and  
1135 Integrated Network Analyses Reveal New Insights into the Systems Relationships between Metabolites,  
1136 Structural Genes, and Transcriptional Regulators in Developing Grape Berries (*Vitis vinifera* L.) Exposed  
1137 to Water Deficit. *Front Plant Sci.* 8:11242017;
- 1138 74. Wong DCJ, Matus JT. Constructing Integrated Networks for Identifying New Secondary Metabolic  
1139 Pathway Regulators in Grapevine: Recent Applications and Future Opportunities. *Front Plant Sci.*  
1140 8:5052017;
- 1141 75. Fabres PJ, Collins C, Cavagnaro TR, Rodríguez-López CM. A Concise Review on Multi-Omics Data  
1142 Integration for Terroir Analysis in *Vitis vinifera*. *Front Plant Sci.* 8:10652017;
- 1143 76. Huang S, Chaudhary K, Garmire LX. More Is Better: Recent Progress in Multi-Omics Data  
1144 Integration Methods. *Front Genet.* 8:842017;
- 1145 77. Stein O'Brien GL, Arora R, Culhane AC, Favorov AV, Garmire LX, Greene CS, et al.. Enter the  
1146 Matrix: Factorization Uncovers Knowledge from Omics. *Trends Genet.* 34:790-8052018;
- 1147 78. Fox J, Friendly M, Weisberg S. Hypothesis tests for multivariate linear models using the car package.  
1148 *R J. Citeseer.* 5:39-522013;
- 1149 79. R Core Team. R: A language and environment for statistical computing. Vienna, Austria;

- 1150 [80. Lenth R, Singmann H, Love J, Others. Emmeans: Estimated marginal means, aka least squares](#)  
1151 [means. \*R package version\*. 12018;](#)
- 1152 [81. Ripley BD. Modern applied statistics with S. Springer;](#)
- 1153 [82. Wickham H. ggplot2: Elegant Graphics for Data Analysis. Springer;](#)
- 1154 [83. Liaw A, Wiener M, Others. Classification and regression by randomForest. \*R news\*. 2:18–222002;](#)
- 1155 [84. Kuhn M. Predictive Modeling with R and the caret Package. \*Google Scholar\*. 2013;](#)
- 1156 [85. Team RC, Others. R foundation for statistical computing. \*Vienna, Austria\*. 32013;](#)
- 1157 [86. Csardi G, Nepusz T, Others. The igraph software package for complex network research.](#)  
1158 [\*InterJournal, complex systems\*. 1695:1–92006;](#)
- 1159 [50. Podani J, Miklós I. Resemblance coefficients and the horseshoe effect in principal coordinates](#)  
1160 [analysis. \*Ecology\*. Wiley; 83:3331–432002;](#)
- 1161 [51. Degu A, Hochberg U, Sikron N, Venturini L, Buson G, Ghan R, et al.. Metabolite and transcript](#)  
1162 [profiling of berry skin during fruit development elucidates differential regulation between Cabernet](#)  
1163 [Sauvignon and Shiraz cultivars at branching points in the polyphenol pathway. \*BMC Plant Biol\*.](#)  
1164 [14:1882014;](#)
- 1165 [52. Anesi A, Stocchero M, Dal Santo S, Commisso M, Zenoni S, Ceoldo S, et al.. Towards a scientific](#)  
1166 [interpretation of the terroir concept: plasticity of the grape berry metabolome. \*BMC Plant Biol\*.](#)  
1167 [15:1912015;](#)
- 1168 [53. Cuadros-Inostroza A, Ruíz-Lara S, González E, Eckardt A, Willmitzer L, Peña-Cortés H. GC-MS](#)  
1169 [metabolic profiling of Cabernet Sauvignon and Merlot cultivars during grapevine berry development and](#)  
1170 [network analysis reveals a stage- and cultivar-dependent connectivity of primary metabolites.](#)  
1171 [\*Metabolomics\*. 12:392016;](#)
- 1172 [54. Dal Santo S, Fasoli M, Negri S, D’Inca E, Vicenzi N, Guzzo F, et al.. Plasticity of the Berry Ripening](#)  
1173 [Program in a White Grape Variety. \*Front Plant Sci\*. 7:9702016;](#)
- 1174 [55. Zamboni A, Di Carli M, Guzzo F, Stocchero M, Zenoni S, Ferrarini A, et al.. Identification of putative](#)  
1175 [stage-specific grapevine berry biomarkers and omics data integration into networks. \*Plant Physiol\*.](#)  
1176 [154:1439–592010;](#)
- 1177 [56. Dal Santo S, Tornielli GB, Zenoni S, Fasoli M, Farina L, Anesi A, et al.. The plasticity of the](#)  
1178 [grapevine berry transcriptome. \*Genome Biol\*. 14:r542013;](#)
- 1179 [57. Chitwood DH, Rundell SM, Li DY, Woodford OL, Yu TT, Lopez JR, et al.. Climate and](#)  
1180 [Developmental Plasticity: Interannual Variability in Grapevine Leaf Morphology. \*Plant Physiol\*.](#)  
1181 [170:1480–912016;](#)
- 1182 [58. Chitwood DH, Mullins J, Migicovsky Z, Frank M, VanBuren R, Londo JP. Vein-to-blade ratio is an](#)  
1183 [allometric indicator of climate-induced changes in grapevine leaf size and shape. \*bioRxiv\*.](#)
- 1184 [59. Bravdo B. EFFECT OF MINERAL NUTRITION AND SALINITY ON GRAPE PRODUCTION](#)  
1185 [AND WINE QUALITY. \*Acta Horticulturae\*. 512:23–302000;](#)

- 1186 [60. Brunetto G, Melo GWBDE, Toselli M, Quartieri M, Tagliavini M. The role of mineral nutrition on](#)  
1187 [yields and fruit quality in grapevine, pear and apple. \*Rev Bras Frutic. FapUNIFESP \(SciELO\)\*; 37:1089–](#)  
1188 [1042015;](#)
- 1189 [61. Gautier A, Cookson SJ, Hevin C, Vivin P, Lauvergeat V, Mollier A. Phosphorus acquisition](#)  
1190 [efficiency and phosphorus remobilization mediate genotype-specific differences in shoot phosphorus](#)  
1191 [content in grapevine. \*Tree Physiol. Oxford University Press \(OUP\)\*; 38:1742–512018;](#)
- 1192 [62. Canas S, Assunção M, Brazão J, Zanol G, Eiras-Dias JE. Phenolic compounds involved in grafting](#)  
1193 [incompatibility of \*Vitis\* spp: development and validation of an analytical method for their quantification.](#)  
1194 [\*Phytochem Anal.\* 26:1–72015;](#)
- 1195 [63. Prodhomme D, Valls Fonayet J, Hévin C, Franc C, Hilbert G, de Revel G, et al.. Metabolite profiling](#)  
1196 [during graft union formation reveals the reprogramming of primary metabolism and the induction of](#)  
1197 [stilbene synthesis at the graft interface in grapevine. \*BMC Plant Biol.\* 19:5992019;](#)
- 1198 [64. Migicovsky Z, Sawler J, Money D, Eibach R, Miller AJ, Luby JJ, et al.. Genomic ancestry estimation](#)  
1199 [quantifies use of wild species in grape breeding. \*BMC Genomics.\* 17:4782016;](#)
- 1200 [65. Vitulo N, Forcato C, Carpinelli EC, Telatin A, Campagna D, D'Angelo M, et al.. A deep survey of](#)  
1201 [alternative splicing in grape reveals changes in the splicing machinery related to tissue, stress condition](#)  
1202 [and genotype. \*BMC Plant Biol.\* 14:992014;](#)
- 1203 [66. Harris ZN, Kovacs LG, Londo JP. RNA-seq-based genome annotation and identification of long-](#)  
1204 [noncoding RNAs in the grapevine cultivar “Riesling.” \*BMC Genomics.\* BioMed Central; 18:9372017;](#)
- 1205 [67. Williams BR, Edwards CE, Kwasniewski MT, Miller AJ. Epigenomic patterns reflect irrigation and](#)  
1206 [grafting in the grapevine clone ‘Chambourcin’. \*bioRxiv.\* Cold Spring Harbor Laboratory; 2020;](#)
- 1207 [68. Marasco R, Rolli E, Fusi M, Michoud G, Daffonchio D. Grapevine rootstocks shape underground](#)  
1208 [bacterial microbiome and networking but not potential functionality. \*Microbiome.\* 6:32018;](#)
- 1209 [69. Swift JF, Hall ME, Harris ZN, Kwasniewski MT, Miller AJ. Grapevine microbiota reflect diversity](#)  
1210 [among compartments and complex interactions within and among root and shoot systems. \*bioRxiv.\*](#)
- 1211 [70. Palumbo MC, Zenoni S, Fasoli M, Massonnet M, Farina L, Castiglione F, et al.. Integrated network](#)  
1212 [analysis identifies fight-club nodes as a class of hubs encompassing key putative switch genes that induce](#)  
1213 [major transcriptome reprogramming during grapevine development. \*Plant Cell. Am Soc Plant Biol;\*](#)  
1214 [26:4617–352014;](#)
- 1215 [71. Savoi S, Wong DCJ, Arapitsas P, Miculan M, Bucchetti B, Peterlunger E, et al.. Transcriptome and](#)  
1216 [metabolite profiling reveals that prolonged drought modulates the phenylpropanoid and terpenoid](#)  
1217 [pathway in white grapes \(\*Vitis vinifera\* L.\). \*BMC Plant Biol.\* 16:672016;](#)
- 1218 [72. Savoi S, Wong DCJ, Degu A, Herrera JC, Bucchetti B, Peterlunger E, et al.. Multi-Omics and](#)  
1219 [Integrated Network Analyses Reveal New Insights into the Systems Relationships between Metabolites,](#)  
1220 [Structural Genes, and Transcriptional Regulators in Developing Grape Berries \(\*Vitis vinifera\* L.\) Exposed](#)  
1221 [to Water Deficit. \*Front Plant Sci.\* 8:11242017;](#)
- 1222 [73. Wong DCJ, Matus JT. Constructing Integrated Networks for Identifying New Secondary Metabolic](#)  
1223 [Pathway Regulators in Grapevine: Recent Applications and Future Opportunities. \*Front Plant Sci.\*](#)  
1224 [8:5052017;](#)

- 1225 [74. Fabres PJ, Collins C, Cavagnaro TR, Rodríguez López CM. A Concise Review on Multi-Omics Data](#)  
1226 [Integration for Terroir Analysis in \*Vitis vinifera\*. \*Front Plant Sci.\* 8:10652017;](#)
- 1227 [75. Huang S, Chaudhary K, Garmire LX. More Is Better: Recent Progress in Multi-Omics Data](#)  
1228 [Integration Methods. \*Front Genet.\* 8:842017;](#)
- 1229 [76. Stein-O'Brien GL, Arora R, Culhane AC, Favorov AV, Garmire LX, Greene CS, et al.. Enter the](#)  
1230 [Matrix: Factorization Uncovers Knowledge from Omics. \*Trends Genet.\* 34:790–8052018;](#)
- 1231 [77. Fox J, Friendly M, Weisberg S. Hypothesis tests for multivariate linear models using the car package.](#)  
1232 [\*R J. Citeseer;\* 5:39–522013;](#)
- 1233 [78. R Core Team. \*R: A language and environment for statistical computing.\* Vienna, Austria;](#)
- 1234 [79. Lenth R, Singmann H, Love J, Others. Emmeans: Estimated marginal means, aka least-squares](#)  
1235 [means. \*R package version.\* 12018;](#)
- 1236 [80. Ripley BD. \*Modern applied statistics with S.\* Springer;](#)
- 1237 [81. Wickham H. \*ggplot2: Elegant Graphics for Data Analysis.\* Springer;](#)
- 1238 [82. Liaw A, Wiener M, Others. Classification and regression by randomForest. \*R news.\* 2:18–222002;](#)
- 1239 [83. Kuhn M. Predictive Modeling with R and the caret Package. \*Google Scholar.\* 2013;](#)
- 1240 [84. Team RC, Others. \*R foundation for statistical computing.\* Vienna, Austria. 32013;](#)
- 1241 [85. Csardi G, Nepusz T, Others. The igraph software package for complex network research.](#)  
1242 [\*InterJournal, complex systems.\* 1695:1–92006;](#)

1243

Figure 1

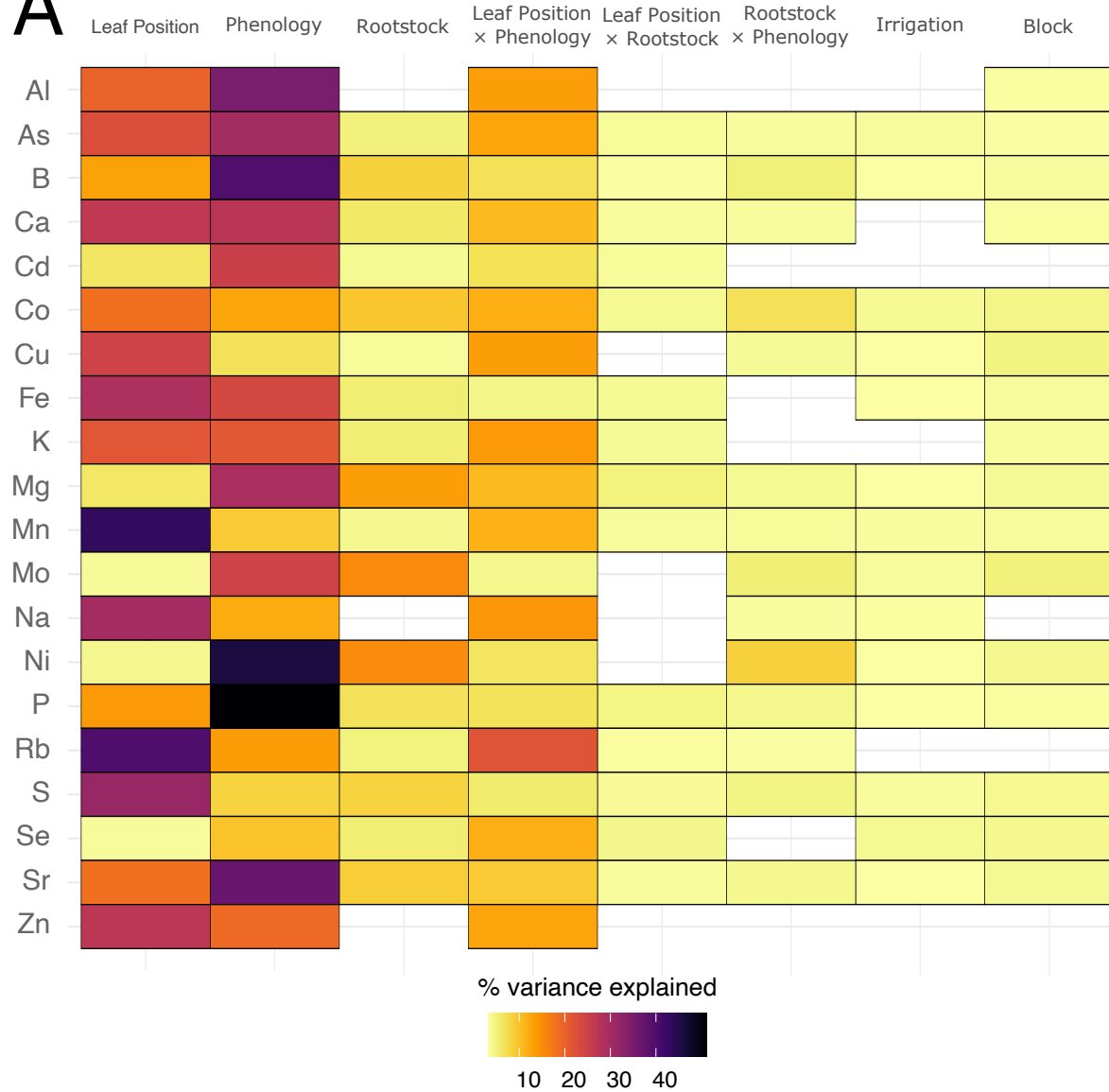
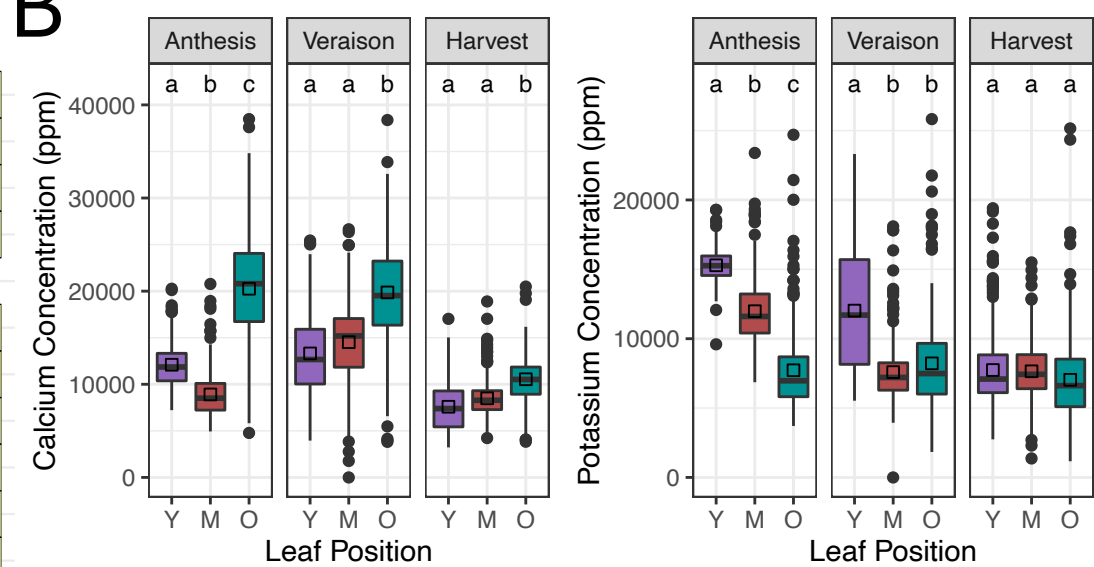
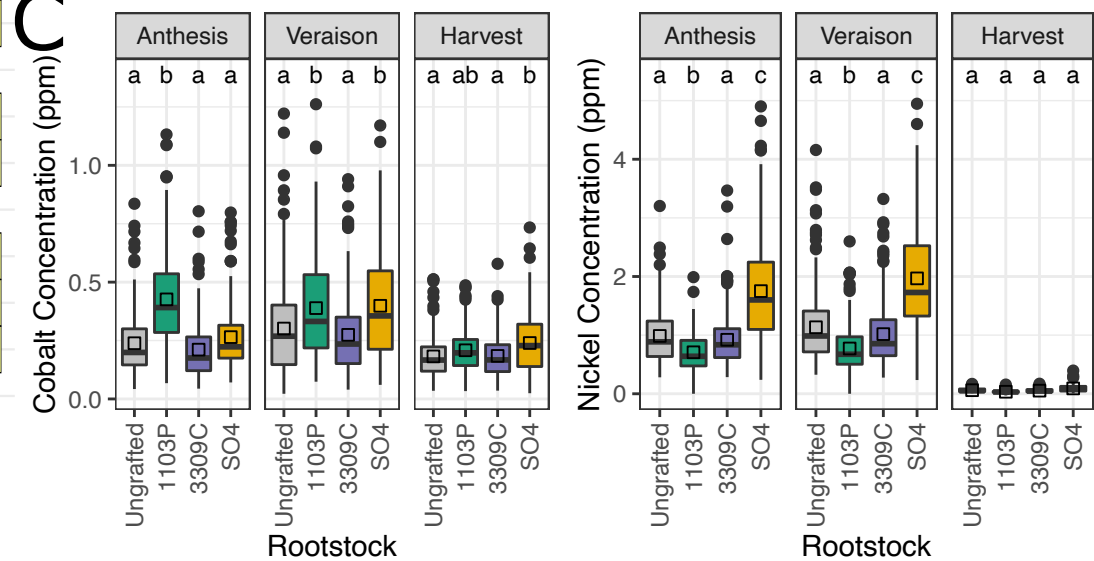
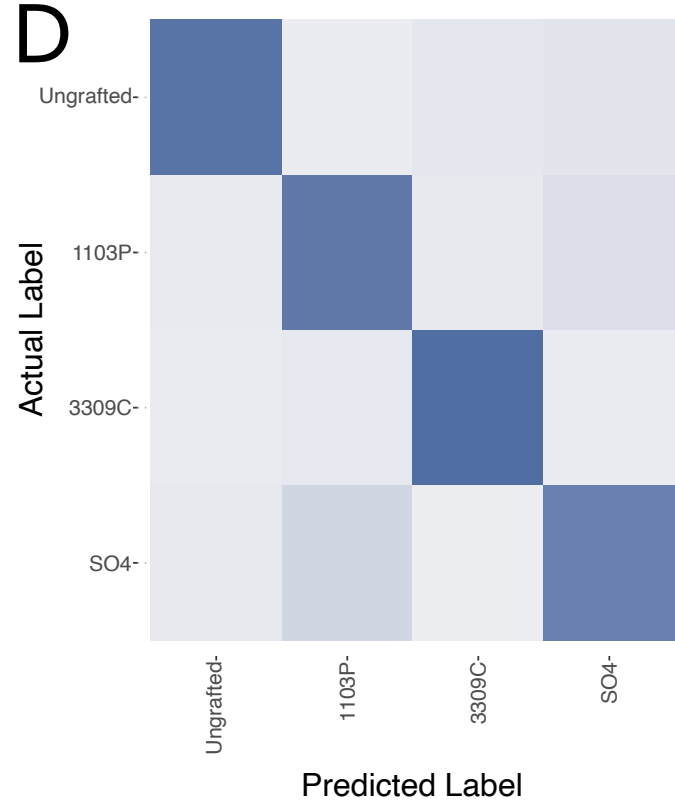
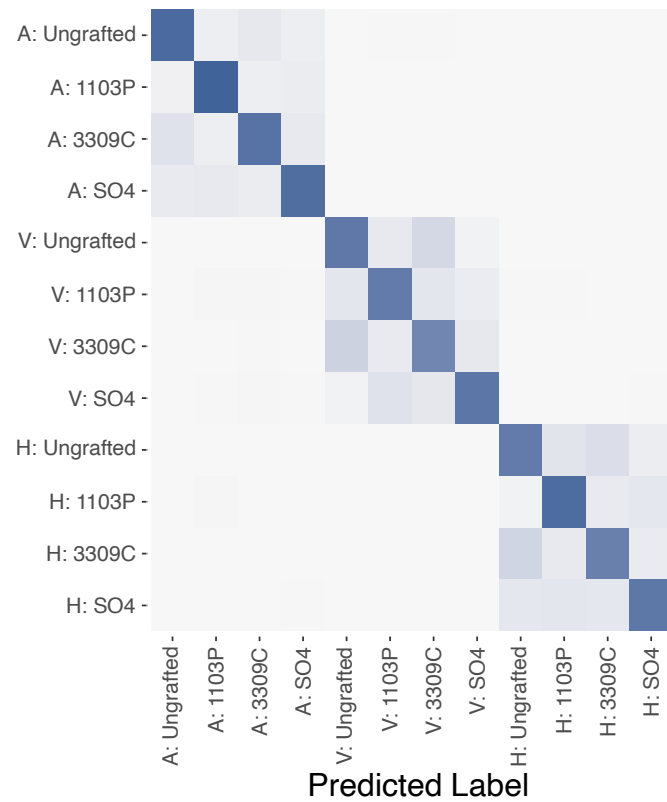
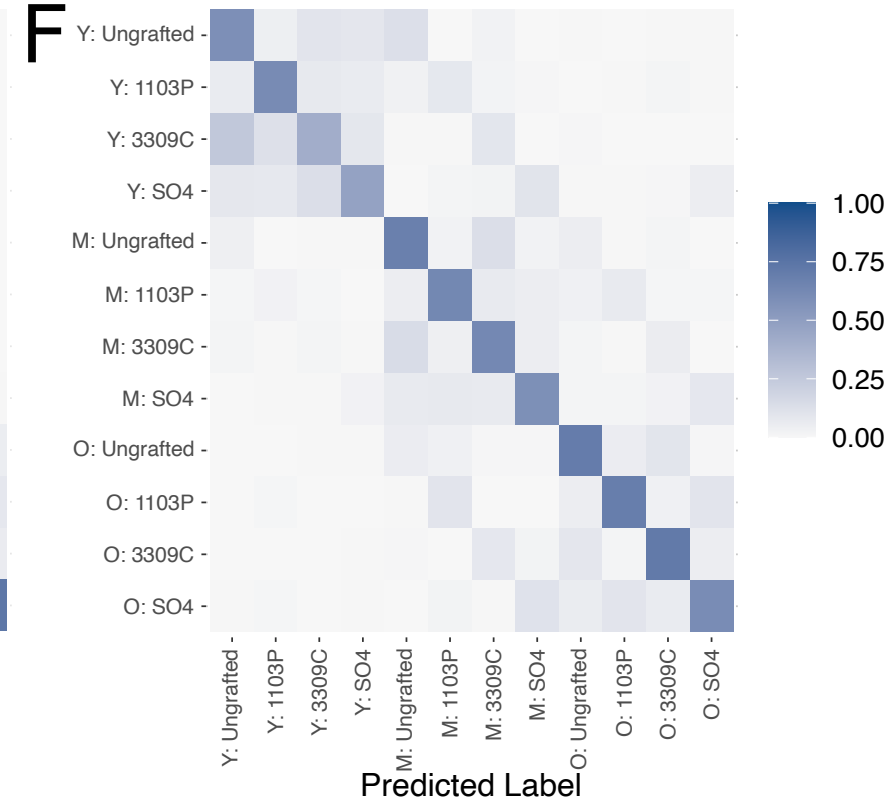
**B****C****D****E****F**

Figure 2

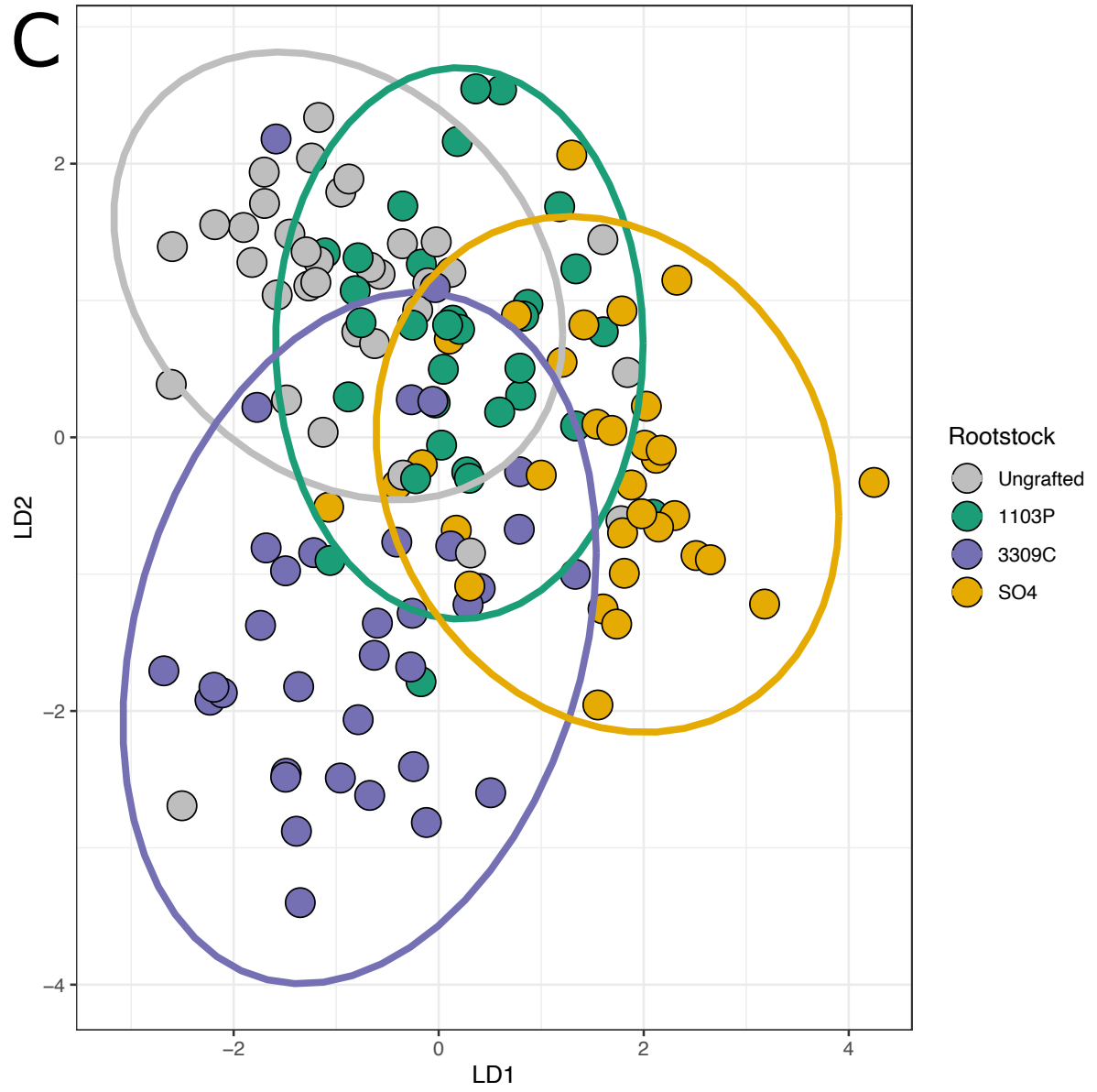
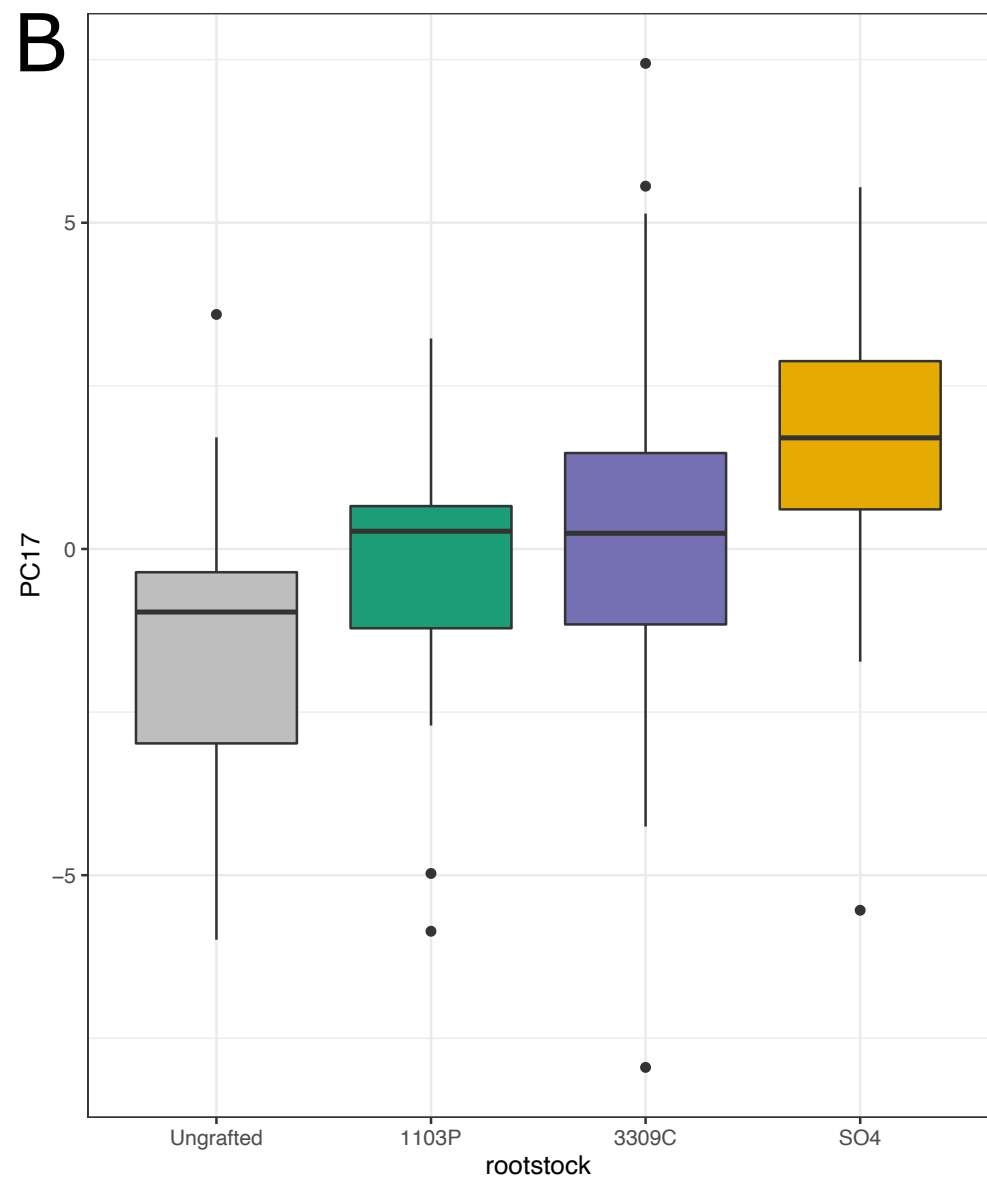
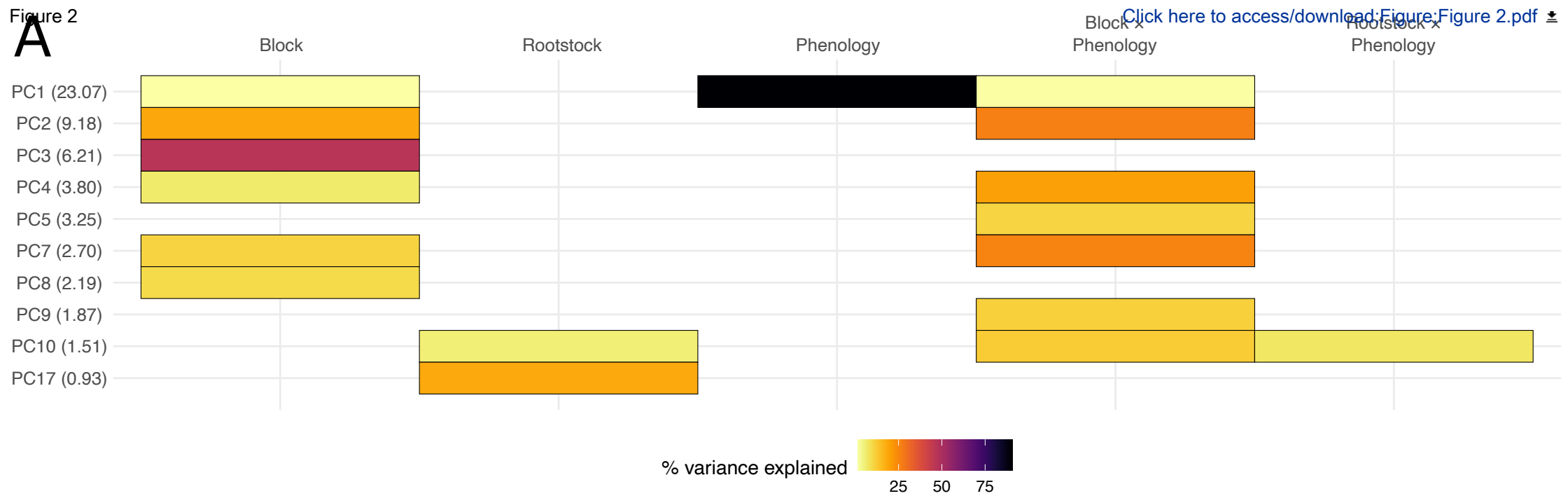


Figure 3

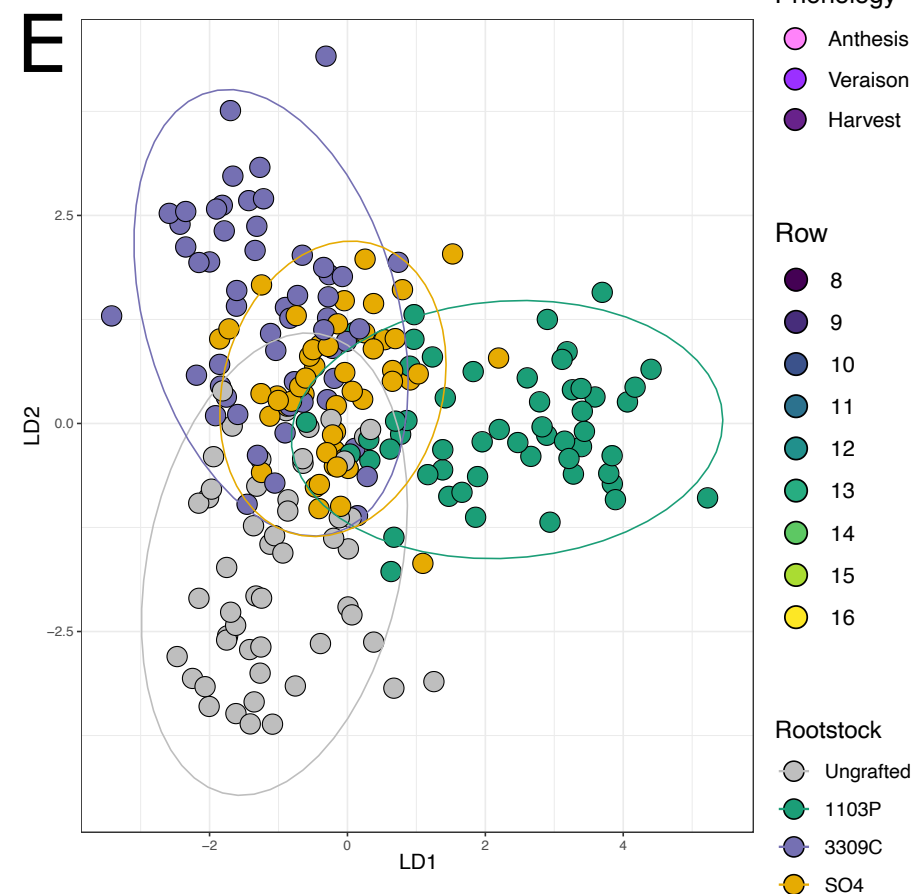
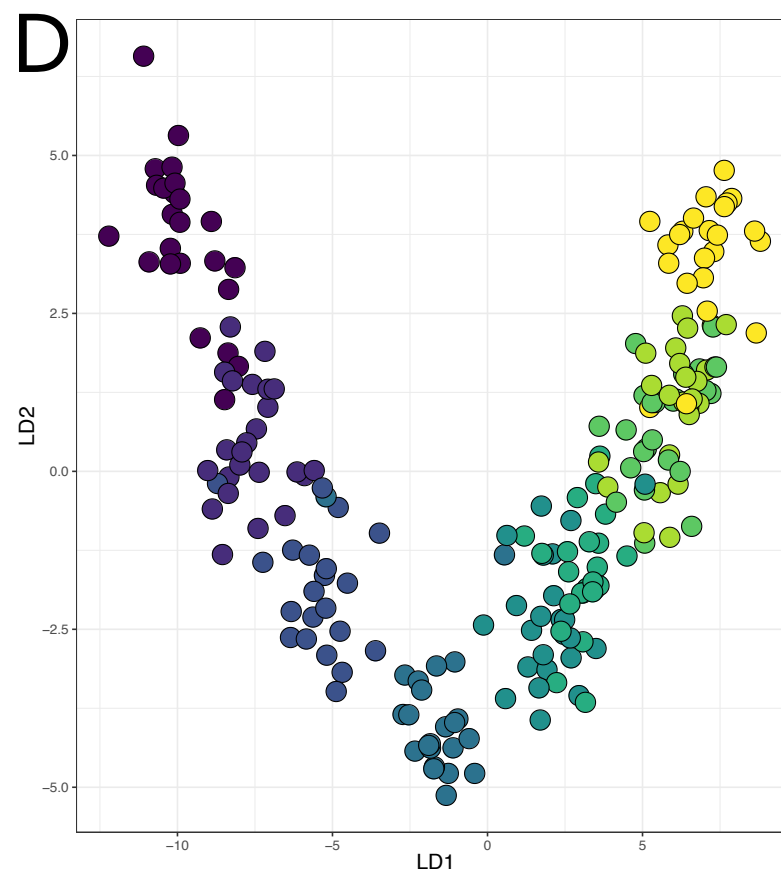
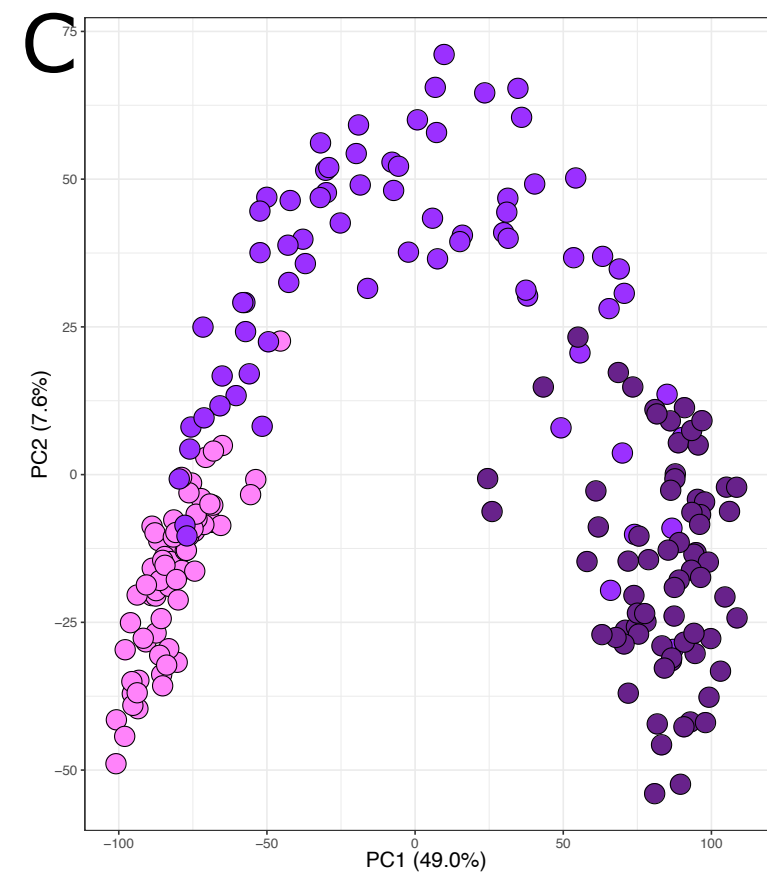
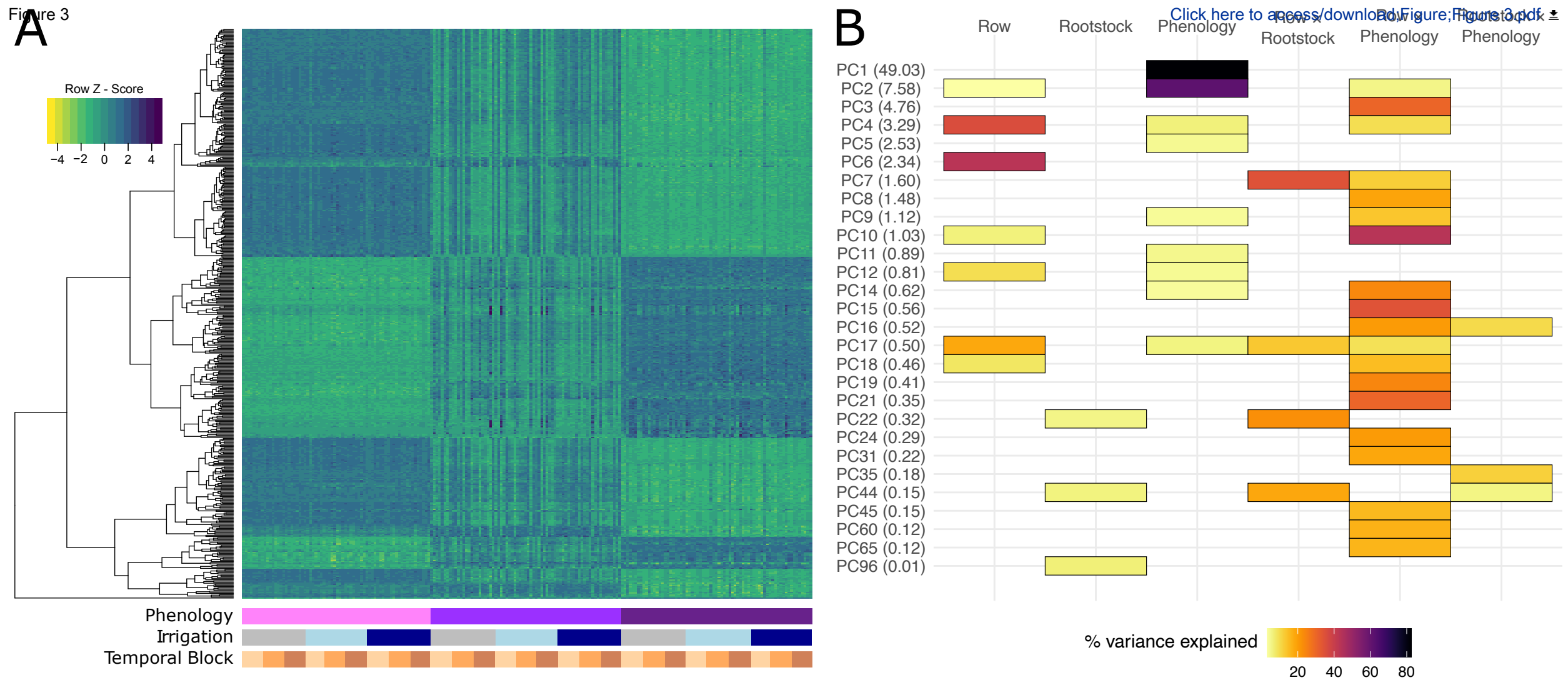
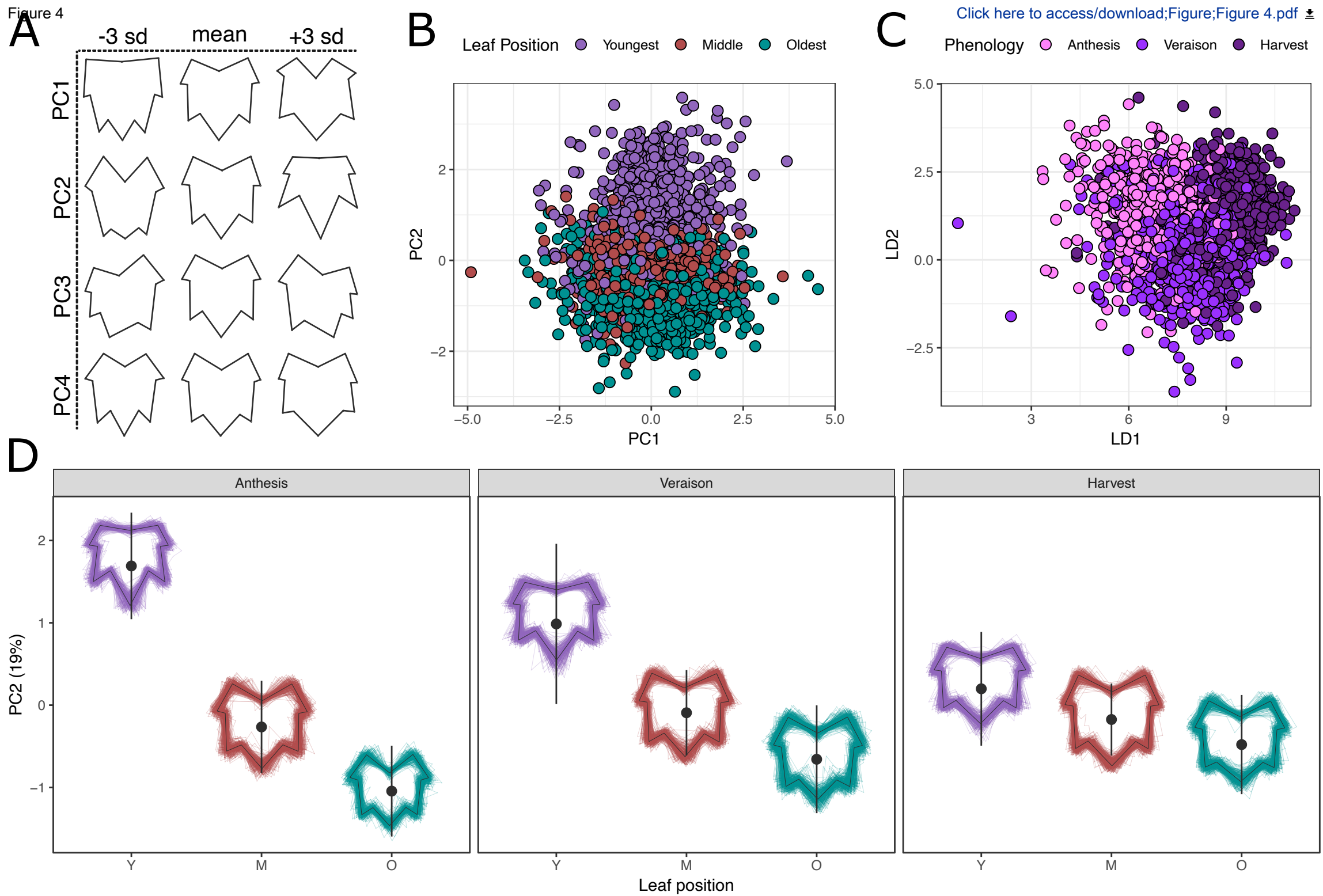




Figure 4



[Click here to access/download;Figure;Figure 4.pdf](#)

Figure 5

[Click here to access/download;Figure;Figure 5.pdf](#)

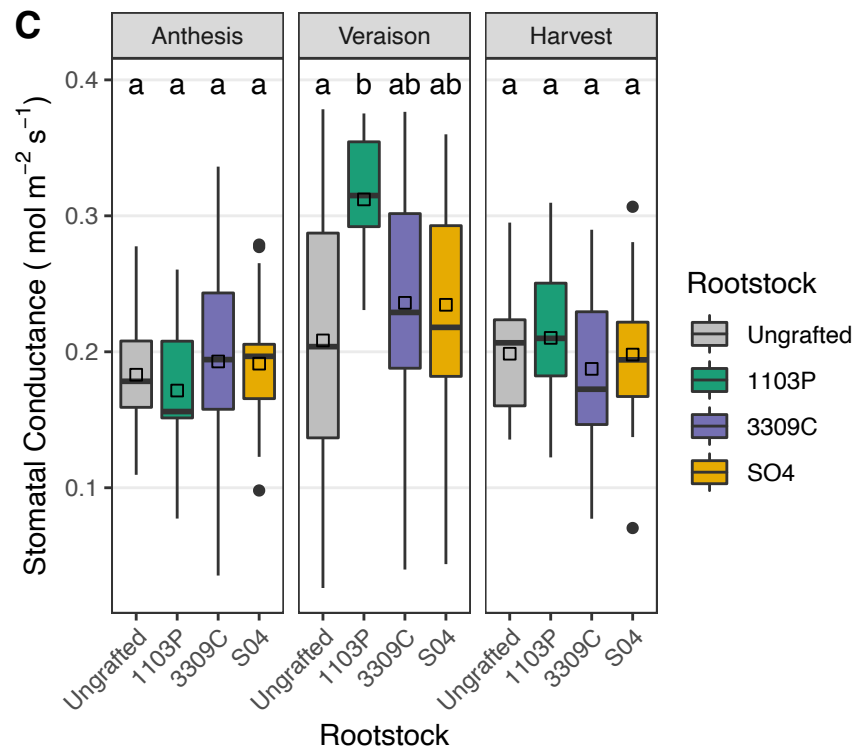
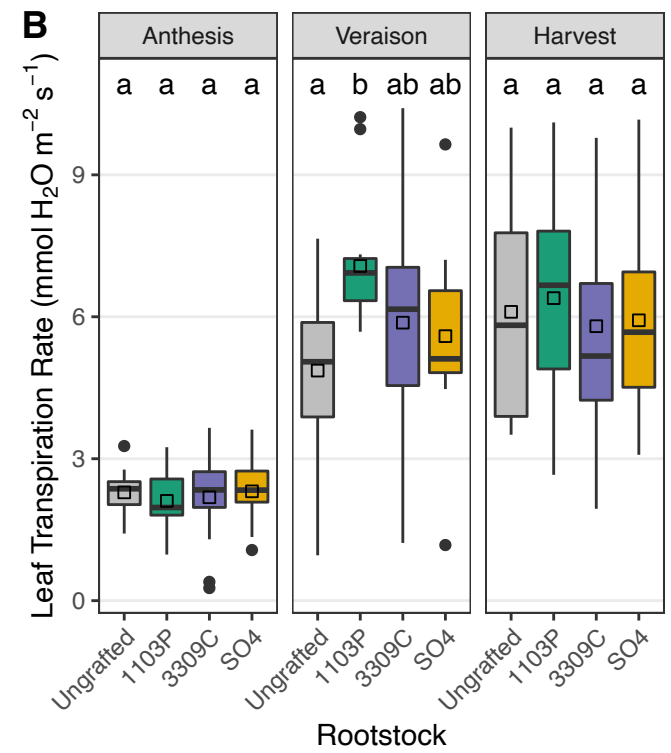
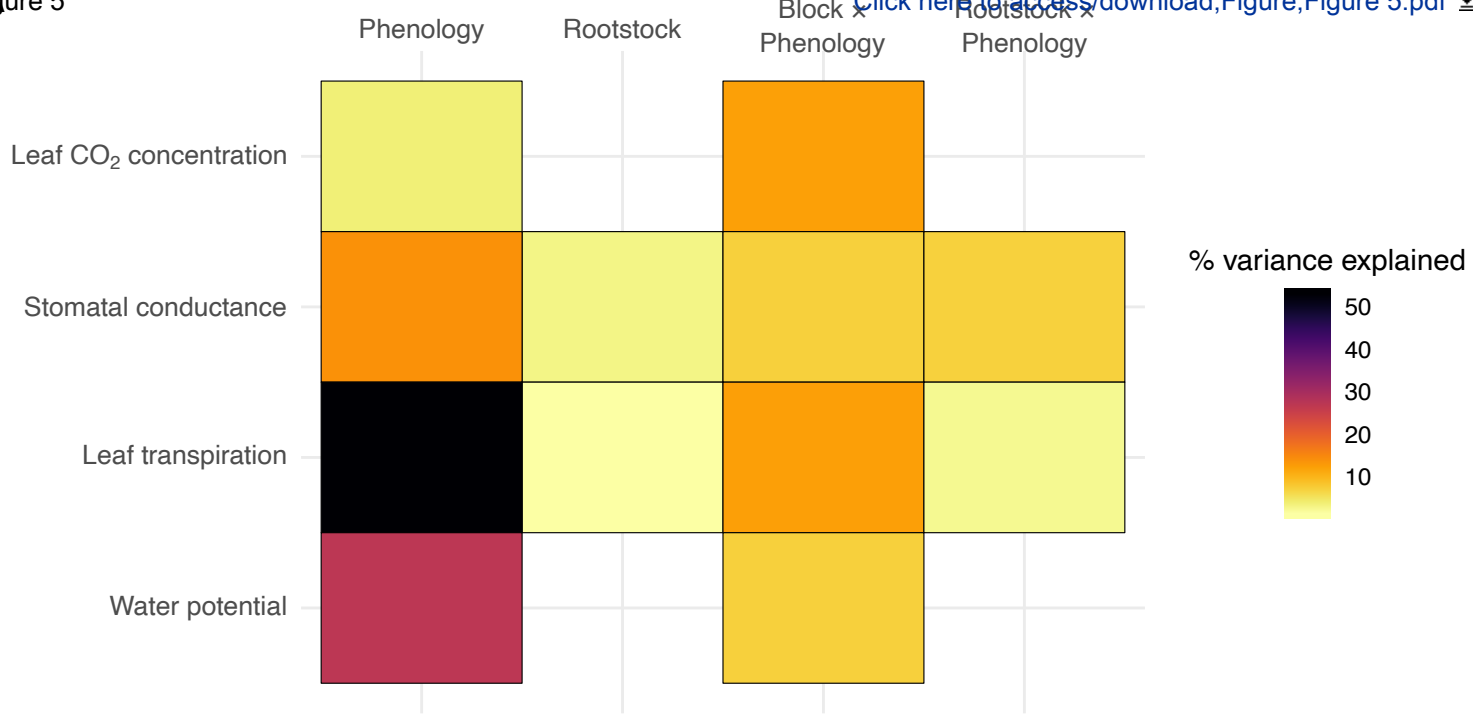
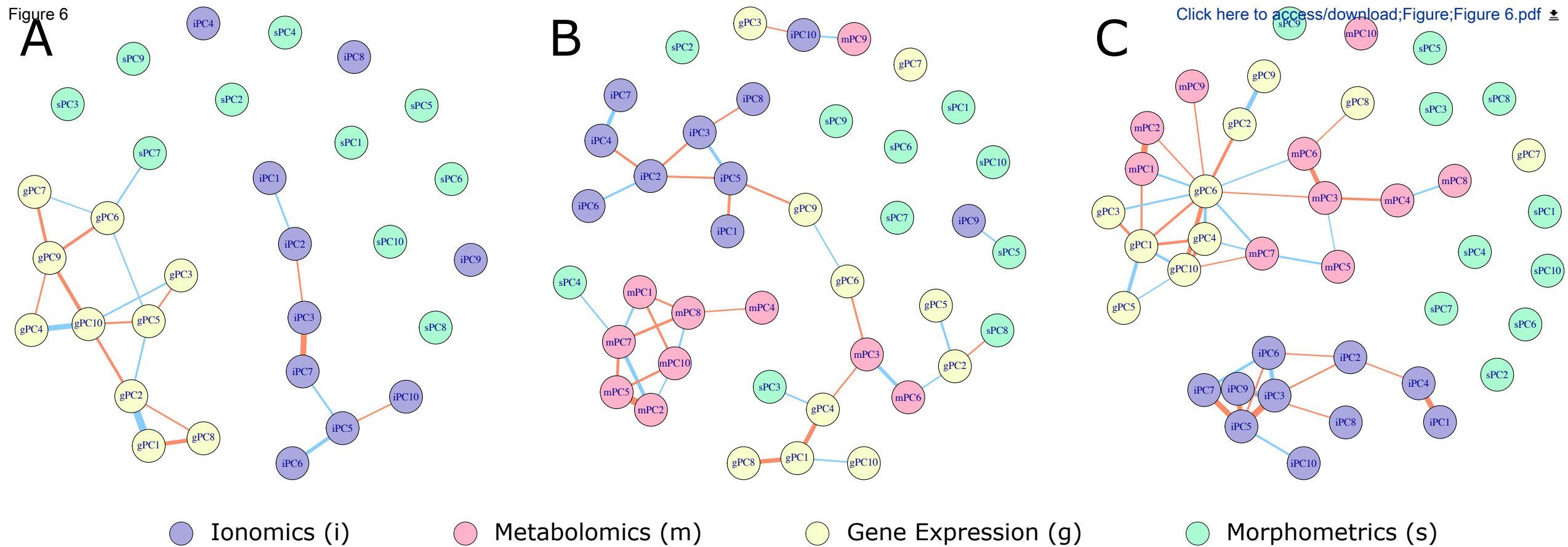


Figure 6



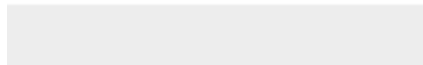


Click here to access/download  
**Supplementary Material**  
Supplemental Figure 1.pdf





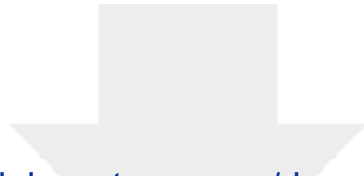
Click here to access/download  
**Supplementary Material**  
Supplemental Figure 2.pdf



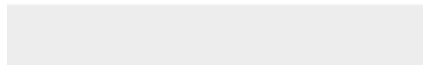


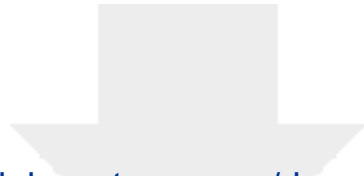
Click here to access/download  
**Supplementary Material**  
Supplemental Figure 3.pdf



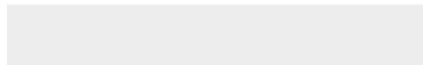


Click here to access/download  
**Supplementary Material**  
Supplemental Figure 4.pdf





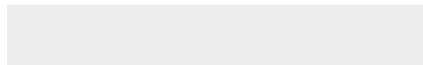
Click here to access/download  
**Supplementary Material**  
Supplemental Figure 5.pdf





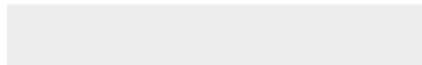



Click here to access/download  
**Supplementary Material**  
Supplemental Figure 6.pdf






Click here to access/download  
**Supplementary Material**  
Supplemental Figure 7.pdf





Click here to access/download  
**Supplementary Material**  
Supplemental Note 1.pdf



Dr. Nicole Nogoy,

We are happy to re-submit our revised manuscript (GIGA-D-21-00137) for review. Again, we would like to thank the reviewers for the careful review of the manuscript and thoughtful comments.

We have made changes to the manuscript in order to address the comments by the reviewers. Most notably, we included comments in the manuscript to address potential intrinsic features of the rootstock that might be driving the changes we saw in the ionome, and we addressed our tradeoff between sample number and read depth for the RNAseq analyses.

In addition, we responded to comments by reviewers 1 and 4 about integrative analyses, typos, and proper data/script placement. In the response below, we also respond to editor comments to express our willingness to share data and scripts as broadly as is needed.

We appreciate the time that everyone has spent looking at this manuscript, and we thank the reviews and editor for their hard work so far. We look forward to hearing back.

Best,  
Zachary N Harris and Allison J Miller

Black Text = Reviewer Comments

Grey Text = Author Response

Note to all: Microsoft Word on macOS does not allow correct continuous line numbering with "track changes" on. All referenced line numbers were identified such that they were continuous. If line numbers appear way off, try changing "All Markup" to "Simple Markup" under the Review tab to align the line numbers.

All revisions from this round are labelled Revision\_2.

## **Editor Comments:**

With regards to Reviewer #4 comments and Github - if the manuscript is deemed acceptable for publication, GigaScience will always take snapshots and host that, along with other supporting data and metadata under a CC0 license. So despite the reviewer's concern about GitHub not being a permanent repository, there will be copies permanent in our open repository, GigaDB.

Response: We thank the editor for their work on this manuscript. We are happy to have additional copies of all of our scripts and data sets hosted redundantly across multiple repositories. Our intention with GitHub was to store the analysis scripts as permanent versions of record. As we do not come from software development, we were using GitHub as a convenient home rather than as a live repository for ongoing projects. One additional note: we uploaded all metabolomics data to Metabolites, but have not received a response from that submission. We would be happy to store an additional copy on GigaDB, if appropriate.

## **Reviewer 1:**

Relevant methodological information that was missing from the previous submission has been added to the revised manuscript by Harris and co-workers, which enables a more conscious interpretation of the results. Experimental limitations and external sources of variation have also been considered when discussing the results. In addition, cross-check of expected expression profiles for a selection of genes has been included as a validation of the RNA-seq experiment reliability.

Response: We thank the reviewer for their careful review and re-review of the manuscript. Comments made by reviewers have considerably strengthened the manuscript and we really appreciate it.

Considering all the information, despite a huge multilevel dataset was generated, its value is limited by experimental design deficiencies recognized by the authors (e.g.: only one year of study under field conditions, noise of environmental/circadian variation during extensive physiological phenotyping and RNA-seq sampling throughout relatively

long periods of the day, theoretically low power of the RNA-seq experiment due to relatively low read depth and low replication in some comparisons with only two replicates). Altogether, the manuscript is mostly descriptive of general differences rather than conclusive. Some of the main observations have already been documented before, such as the idea that rootstock genotype affects scion leaf phenotypes. Regardless, in the current version of the manuscript, the study and its limitations are fairly presented by the authors in a manner that would be acceptable for publication if the journal considers the dataset of value in spite of these experimental limitations. Besides this general concern, I would only have a few minor comments to this version:

1. The dataset might still be undermined as only general descriptive differences are presented as conclusions, but nothing about their possible origin is mentioned. For instance, what are the known intrinsic features of the compared rootstocks according to the bibliography that could determine the observed differences in ionic composition? How could these rootstock-determined differences in ion accumulation affect vine performance? Similar questions would arise for other differences observed.

- Response: Thank you for this comment, and we share a strong interest in understanding intrinsic features of rootstocks that affect the observed differences in the grafted scion. Studies that begin to get at these questions are underway within our research team now, but unfortunately are not completed and not included in this manuscript. To address the reviewer comments here, we specified that, especially in the case of the ionome, the differences are likely due to the genetics/ pedigree of the rootstock on [L521-523](#). Additional comments added in the last round of revision explain how we are presently unsure how individual ions map to aspects of vine performance. We know even less about the other phenotypes. Future analyses using the data set we presented, additional data that were beyond the scope of leaf phenotyping, and future data can and should address this type of question.

2. It could be more specifically pointed out that lack of DEGs in some RNA-seq comparisons could be due to the experimental limitations (e.g.: low replication and 4.1 M read depth below the minimum recommended 5 M) rather than to a real lack of effect of rootstock genotype.

- Response: Agreed. We added a note to the Data Description that we opted to sequence more samples at the cost of some read depth which does limit our power to detect some low-expression genes on [L195-196](#). We recognize that replication is low for high order interactions (rootstock:row:phenology) due to only sampling two vines per cell. Because of this low replication, we did not interpret such effects because they would be underpowered. However we sampled 36 cells at each time point for a total of 216 samples (with a few removed for poor

sequencing), so lower order interactions and main effects were derived from much larger pools of clonally replicated samples. Specific details on this can be found in response to Reviewer 2 and 4 in the first revision.

3. The value of including PC covariation networks would be scarce if the results are not reliable enough for interpreting the inter-connection identified between the responsible specific metabolites, ions, genes, etc.

- Response: It's true, and we agree that any issues present in individual data sets will percolate into integrative analyses. Having said that, we are confident in the individual datasets and in our approach using those datasets in PC covariation networks. Focusing on PCs from each modality allowed us to capture the highest levels of variation to see how those PCs relate across modalities. We chose this analysis so that no particular modality was over-weighted and so that we could narrow down where interesting correlations lie such that we can design and craft better future studies. We recognize this approach has limitations, but after exploring many different potential options we felt this was the most appropriate given the data and the questions.

4. Several typos should be corrected in the newly added text.

- Response: We thank the reviewer for the close reading of the text. We have edited the manuscript for typos, grammar, and tense.

## **Reviewer 2:**

I was pleased to review the resubmitted manuscript by Harris and co-workers, who have responded to my original review. The Authors have clarified a number of points regarding the RNAseq experiments including RNA extraction methods, and the tissue type that was used. More information has been added to the methods that would aid reproducibility. Additional statistics have been applied to Figures 1 and 5. Numerous formatting and grammatical changes have been made that improve the readability of the manuscript. Additional supporting references have been provided. While not all of my suggestions were included, I accept the authors responses to my original review. I have no further concerns and recommend the manuscript for publication in GigaScience.

- Response: We thank the reviewer for their careful considerations of our manuscript. The manuscript has been considerably improved thanks to the reviewer's comments.

## **Reviewer 3:**

I found that the Authors clearly improved the ms which might be suitable for publication

- Response: We thank the reviewer for their careful considerations of our manuscript. We especially thank the reviewer for comments on improving figures. The presentation of our work was improved by the reviewer's comments.

#### **Reviewer 4:**

- I saw the editor comments about appropriate data storage, but I disagree with those comments to the authors.
- Github is not a permanent repository and as such it's not true that it's the most appropriate place to share scripts for a publication. It is only suitable as a place for collaboration. As the authors make changes, the version of record for this manuscript will no longer be available, and the authors could delete it at any time. The publication versions should be separately repositied in a permanent repository. In my opinion, if a script is meant to be a version of record and also living, then a link to both the permanent repository and to GitHub can be given.
- I am not sure what is meant by 'large-scale' data. Figshare is a general use repository that I only recommended since the authors already were using it. It can host single files up to 5 gb in size, provides unlimited public space, and provides a DOI. So what exactly is unsuitable?
- Zenodo is another free option, and there is Data Dryad and the Data Commons.
- Response: We thank the reviewer for their careful considerations of our manuscript. We are happy to share our data and scripts in any way requested. Our intention was to use Github as a repository for a version of record, but we recognize that it is not a perfect solution. We are happy that Gigascience will host snapshots so that there is no potential for misuse. If the reviewer would like an additional home for the scripts we would be very happy to do that.